

---

# Is merging worth it? Securely evaluating the information gain for causal dataset acquisition

---

**Jake Fawkes** \*  
University of Oxford  
jake.fawkes@st-hughs.ox.ac.uk

**Lucile Ter-Minassian** \*  
University of Oxford  
lucile.ter-minassian@spc.ox.ac.uk

**Desi Ivanova**  
University of Oxford

**Uri Shalit**  
Technion – Israel Institute of Technology

**Chris Holmes**  
University of Oxford

## Abstract

Merging datasets across institutions is a lengthy and costly procedure, especially when it involves private information. Data hosts may therefore want to prospectively gauge which datasets are most beneficial to merge with, without revealing sensitive information. For causal estimation this is particularly challenging as the value of a merge will depend not only on the reduction in epistemic uncertainty but also the improvement in overlap. To address this challenge, we introduce the first *cryptographically secure* information-theoretic approach for quantifying the value of a merge in the context of heterogeneous treatment effect estimation. We do this by evaluating the *Expected Information Gain* (EIG) and utilising multi-party computation to ensure it can be securely computed without revealing any raw data. As we demonstrate, this can be used with differential privacy (DP) to ensure privacy requirements whilst preserving more accurate computation than naive DP alone. To the best of our knowledge, this work presents the first privacy-preserving method for dataset acquisition tailored to causal estimation. We demonstrate the effectiveness and reliability of our method on a range of simulated and realistic benchmarks. The code is available anonymously.

## 1 Introduction

As the demand for data-driven decision making grows, the question of how to optimally collect data for a given task becomes increasingly important. One of the most popular data collection methods is *data fusion* [11]. This focuses on integrating pre-existing data from different sources in order to increase sample size, reduce sampling variability, and improve statistical power and robustness [16, 37]. However, merging datasets is often a time-consuming and resource-intensive task. This is especially true in sensitive domains such as healthcare, where concerns surrounding privacy, downstream applications, and data security [19, 45, 51] mean long ethical approval procedures are required before undergoing a merge. Given these considerations, practitioners crucially need methodology for determining in advance if a merge is worth it, whilst also complying with privacy requirements [1].

In this work, we focus on data fusion in the context of heterogeneous treatment effect estimation. As a specific example of the problem we consider, imagine a hospital wants to assess the effect of a medical intervention on its patients but finds its own data is insufficient to get accurate estimates. Therefore, it plans to select one of  $K$  local hospitals in which to conduct a follow-up study. As running such a study is expensive and time consuming, the hospital would like to identify *in advance* which

---

\*Shared first authorship

potential dataset would provide the most information upon merging *whilst* complying with privacy regulations. Here, we propose a solution for this problem, allowing for patient outcomes at the other hospitals to be unobserved or simply masked.

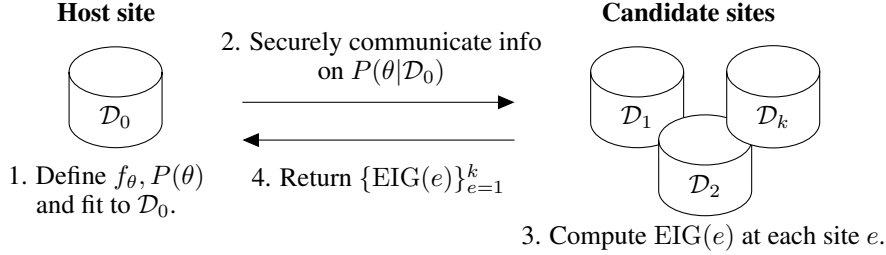


Figure 1: Flow chart depicting the proposed method. In step 1 the *host site* chooses a parameterised model class for the conditional outcome, given by  $f_\theta$  and sets the prior  $P(\theta)$ . They then perform a local Bayesian update, and communicate information on the posterior  $P(\theta|\mathcal{D}_0)$  to the *candidate site* using secure multi party computation. The candidate applies multi party computation once more to privately calculate the Expected Information Gain (EIG) and communicate it back to host. This allows the host to select the best merge out of the potential candidates.

To do this we apply techniques from Bayesian experimental design [12, 40, 53] to quantify the value of a merge in a principled, information theoretic way. Our solution has similarities with standard Bayesian dataset acquisition [33, 43], however in causal contexts data serve an additional, distinct purpose. Specifically acquired data should not only enhance our understanding of the outcome function, but also assist in combating the selection bias that is inherent to causal effect estimation [27] by balancing treatment. Put differently, while generic data fusion aims at reducing the epistemic uncertainty stemming from incomplete knowledge of the outcome, causal estimation also seeks to improve treatment overlap [14, 56], i.e. reducing the epistemic uncertainty for counterfactual outcomes. To resolve this, we make use of favourable parameterisations available in popular Bayesian causal inference methods [2, 23] which allows us to prioritise information gain in the parameters that are relevant for the causal problem, as opposed to gaining information in irrelevant parts of the conditional outcome. We compare our methodology against standard Bayesian dataset acquisition, finding benefits in the causal context.

For privacy, we make use of Secure Multi-Party Computation (MPC)[20, 34, 67]. With this cryptographic protocol, a number of parties can jointly compute the output of a function without revealing their own private input. A classic example is allowing a group of people to find out who is wealthiest without any individual revealing their net worth. In our context it allows the different candidate sites to compute their information gains relative to the initial sites’ data, without anyone having to reveal the content of their dataset. This ensures that the noise required for privacy guarantees can be added at the end of the computation as opposed to the start. As we demonstrate in our experiments section this leads to more accurate computation of statistics.

Our contributions are as follows:

- We propose information-theoretic methods to measure the value of a data merge in the context of heterogeneous treatment effects estimation. Our primary contribution is a novel approach that specifically targets the reduction of entropy in parameters that directly influence the conditional average treatment effect (CATE). Additionally, we also present a standard approach based on expected entropy reduction in all parameters of a conditional outcome model.
- We demonstrate how the former, novel approach may be used with three popular Conditional Average Treatment Effect (CATE) estimators; Bayesian Polynomial Regression [22], Causal Multitask Gaussian Processes [2], and Bayesian Causal Forests [23]. We derive closed form expressions for the expected entropy reduction in the first two models and give a Monte Carlo estimator for Bayesian Causal Forests.
- We provide a privacy protocol for our method based on multi-party computation [67]. This gives us privacy and security guarantees without having to noise the data. For example guaranteeing differential privacy [17] to an arbitrary degree.

- We experimentally validate our methodology across a range of synthetic and semi-synthetic tasks, demonstrating strong agreement between our prospective rankings and the true rankings given by performing the merge. Moreover we find that our proposed methodology to target CATE parameters improves over traditional Bayesian data selection and a number of proposed baselines. Finally we show that the multi party computation protocol incurs minimal loss in accuracy, contrasting this to differential privacy in the linear setting.

## 2 Problem Statement and Notations

### 2.1 Notation

The random variables  $X$ ,  $T$ , and  $Y$  represent the covariates, treatment, and outcomes, with domains  $\mathcal{X}$ ,  $\{0, 1\}$ , and  $\mathcal{Y}$  respectively, and  $\mathbf{x}$ ,  $t$ , and  $y$  denoting realisations of the variables. We let  $\mathcal{D}_e$  be the dataset comprised of elements  $\{\mathbf{x}_i, t_i, y_i\}_{i=1}^{n_e}$ , drawn i.i.d. from a distribution  $P_e(\mathbf{x}, t, y)$ , where  $e \in \{0, \dots, K\}$  indexes the datasets. Vectors of observations in  $\mathcal{D}_e$  are denoted by  $\mathbf{y}_e$  and  $\mathbf{t}_e$ , while  $\mathbf{X}_e$  refers to the data matrix, so that  $\mathbf{y}_e = (y_i)_{i=1}^{n_e}$ ,  $\mathbf{t}_e = (t_i)_{i=1}^{n_e}$ , and  $\mathbf{X}_e = (\mathbf{x}_i)_{i=1}^{n_e}$ . We use potential outcomes [55], so that  $Y(t)$  to represents the outcome resulting from intervening with  $T = t$ .

### 2.2 Objective and Assumptions

Throughout we focus on estimating the *Conditional Average Treatment Effect* (CATE), given by:

$$\tau(\mathbf{x}) = \mathbb{E}[Y(1) - Y(0)|X = \mathbf{x}] \quad (1)$$

To estimate CATE, we begin with an initial dataset,  $\mathcal{D}_0$ , which is referred to as the *host*. Our goal is to accurately estimate CATE with respect to the distribution of this dataset,  $P_0(\mathbf{x})$ . Specifically, we focus on reducing the Precision in Estimation of Heterogeneous Effects (PEHE) [26] given by  $\epsilon_{\text{PEHE}}(f) = \int_{P_0(\mathbf{x})} (\hat{\tau}_f(\mathbf{x}) - \tau(\mathbf{x}))^2 d\mathbf{x}$ , where  $\hat{\tau}_f$  is the CATE model arising the outcome model,  $f$ .

We assume there are a number of potential datasets for merging,  $\mathcal{D}_e$ , which are referred to as the *candidate* sites. We further take that the outcomes are unmeasured or masked in the candidate datasets, and so denote them by  $\mathcal{D}_e = \{\mathbf{x}_i^e, t_i^e, Y_i^e\}_{i=1}^{n_e}$  to show the randomness in  $Y_i^e$ . The goal is to prospectively select which of the candidate datasets  $\mathcal{D}_e$ , would reduce the uncertainty over CATE if we were to measure or unmask the  $Y_i^e$ 's and merge with the host dataset  $\mathcal{D}_0$ .

We assume that datasets are generated according to the Directed Acyclic Graph (DAG) in Figure 2.<sup>2</sup> This implies that  $P(y|\mathbf{x}, t, e)$  is fixed across environments, but both covariate distributions and treatment allocation schemes are free to vary i.e.  $P(\mathbf{x}, t|e)$  can depend on  $e$ . We also assume positivity over the whole population, so that  $\forall \mathbf{x}, 0 < P(T = 1|X = \mathbf{x}) < 1$ . Note this still allows for deterministic treatment assignment within particular hospitals i.e. for any  $\mathbf{x}$ , the corresponding subjects may be systematically treated or untreated in one site, but not across all sites. Adding the consistency assumption (i.e.  $Y(t) = Y$  when  $T = t$ ) to positivity and the causal structure in Figure 2 (which implies no hidden confounders) we have that CATE is identified [50, 54], constant across environments  $e$ , and given by:

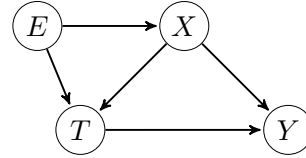


Figure 2: Assumed DAG

$$\begin{aligned} \tau(\mathbf{x}) &= \mathbb{E}[Y|X = \mathbf{x}, T = 1] - \mathbb{E}[Y|X = \mathbf{x}, T = 0] \\ &= \mathbb{E}[Y|X = \mathbf{x}, T = 1, E = e] - \mathbb{E}[Y|X = \mathbf{x}, T = 0, E = e] \end{aligned}$$

## 3 Method

We take a Bayesian approach to modelling the CATE. Specifically, we define  $f_\theta : \mathcal{X} \times \{0, 1\} \rightarrow \mathcal{Y}$  to be a function representing the expected outcome conditional on covariates and treatment, i.e.,  $f_\theta(\mathbf{x}, t)$  seeks to approximate  $\mathbb{E}[Y|X = \mathbf{x}, T = t]$ . We assign a prior distribution  $P(\theta)$ , to the parameters  $\theta$  and denote the conditional likelihood of the outcome given parameters, covariates, and treatment as  $P(Y|\theta, \mathbf{x}, t)$ , which is chosen appropriately based on the type of outcome being modelled. For

<sup>2</sup>We make use of the SWIG framework to combine causal graphical models with potential outcomes. More details can be found in Richardson and Robins [54].

example, we can select a normal likelihood for continuous outcomes, or a Bernoulli likelihood for binary ones. The general form can be written as:

$$Y|f_\theta(\mathbf{x}, t) \sim P(Y|\theta, (\mathbf{x}, t)), \quad \theta \sim P(\theta).$$

Throughout this paper we focus on continuous  $y$  and use a normal likelihood with fixed variance  $\sigma^2$ , meaning that  $P(Y|\mathbf{x}, t, \theta) = \mathcal{N}(Y; f_\theta(\mathbf{x}, t), \sigma^2)$ . CATE is then estimated via the current posterior mean, so that if we have conditioned on data  $\mathcal{D}$  our estimate is  $\hat{\tau}(\mathbf{x}) = \mathbb{E}_{\theta \sim P(\theta|\mathcal{D})}[f_\theta(\mathbf{x}, 1) - f_\theta(\mathbf{x}, 0)]$ .

### 3.1 Quantifying Data Merge Utility through Expected Information Gain

In order to quantify the value of a data merge, we draw inspiration from Bayesian experimental design [12, 53]. Bayesian experimental design applies information theory to provide a measure of what performing a particular experiment would tell us about a parameter of interest, relative to our current beliefs about the parameter value. In our context, the ‘design’ of the experiment corresponds to choosing a dataset  $\mathcal{D}_e$ , and the outcome is observing  $\{Y_i^e\}_{i=1}^{n_e}$ . The value of an experiment is quantified via the expected information gain (EIG) [40], which measures the expected reduction in uncertainty in the parameters, as measured by Shannon entropy, when moving from the post host posterior,  $P(\theta|\mathcal{D}_0)$  to the post merge posterior,  $P(\theta|\mathcal{D}_0, \mathcal{D}_e)$ . Mathematically, this is expressed as:

$$\text{EIG}_{\theta|\mathcal{D}_0}(e) = \mathbb{E}_{P(\mathbf{y}_e|\mathbf{X}_e, \mathbf{t}_e, \mathcal{D}_0)} [H[P(\theta|\mathcal{D}_0)] - H[P(\theta|\mathcal{D}_0, \mathcal{D}_e)]],$$

where  $P(\mathbf{y}_e|\mathbf{X}_e, \mathbf{t}_e, \mathcal{D}_0) = \mathbb{E}_{P(\theta|\mathcal{D}_0)}[P(\mathbf{y}_e|\theta, \mathbf{X}_e, \mathbf{t}_e)]$  is the Bayesian marginal distribution of the outcomes, and  $H[P(\cdot)] = -\mathbb{E}_{P(\cdot)}[\log[P(\cdot)]]$  is the Shannon entropy.

The EIG is equivalent to the mutual information between parameters and outcomes under the candidate design [40], which allows us to write it in its symmetrical form as the expected log ratio of the likelihood to the marginal likelihood:

$$\text{EIG}_{\theta|\mathcal{D}_0}(e) = \mathbb{E}_{P(\theta|\mathcal{D}_0)} [H[P(\mathbf{y}_e|\mathbf{X}_e, \mathbf{t}_e, \mathcal{D}_0)] - H[P(\mathbf{y}_e|\theta, \mathbf{X}_e, \mathbf{t}_e)]] \quad (2)$$

$$= \mathbb{E}_{P(\mathbf{y}_e, \theta|\mathbf{X}_e, \mathbf{t}_e, \mathcal{D}_0)} \left[ \log \frac{P(\mathbf{y}_e|\theta, \mathbf{X}_e, \mathbf{t}_e)}{P(\mathbf{y}_e|\mathbf{X}_e, \mathbf{t}_e, \mathcal{D}_0)} \right]. \quad (3)$$

This is also known as Bayesian Active Learning by Disagreement (BALD) in the active learning literature [28]. For certain classes of models, such as polynomial regression or Gaussian processes, the EIG is available in closed form [58]. In other cases if the likelihood function is analytically available, we can approximate (3) using nested Monte Carlo [21, 52] as follows:

$$\widehat{\text{EIG}}_{\theta|\mathcal{D}_0}^{\text{NMC}}(e) = \frac{1}{N} \sum_{i=1}^N \log \frac{P(\mathbf{y}_e^{(i)}|\theta^{(i)}, \mathbf{X}_e, \mathbf{t}_e)}{\frac{1}{M_1} \sum_{j=1}^{M_1} P(\mathbf{y}_e^{(i)}|\theta'_j, \mathbf{X}_e, \mathbf{t}_e)}, \text{ where } \begin{cases} \theta^{(i)} \sim P(\theta|\mathcal{D}_0), \\ \mathbf{y}_e^{(i)} \sim P(\mathbf{y}_e|\theta^{(i)}, \mathbf{X}_e, \mathbf{t}_e) \\ \theta'_j \sim P(\theta|\mathcal{D}_0) \end{cases} \quad (4)$$

Note that since we assume a normal likelihood, we can construct a Rao-Blackwellised estimator by analytically computing the entropy of the likelihood in (2) to give:

$$\widehat{\text{EIG}}_{\theta|\mathcal{D}_0}^{\text{RB}}(e) = -\frac{1}{N} \sum_{i=1}^N \log \left( \frac{1}{M_1} \sum_{j=1}^{M_1} P(\mathbf{y}_e^{(i)}|\mathbf{X}_e, \mathbf{t}_e, \theta'_j) \right) - \frac{n_e}{2} (1 + \log(2\pi\sigma^2)).$$

A detailed algorithm for both estimators is given in Appendix A.1. Rainforth et al. [52] showed that such nested estimators converge to the expected information gain at rate  $\mathcal{O}((N^{-1} + cM_1^{-2})^{\frac{1}{2}})$ .

Using these estimators we can gauge the value of a merge before observing outcomes  $\{Y_i^e\}_{i=1}^{n_e}$  in the dataset  $\mathcal{D}_e$ . However, whilst this does provide us with information gain on the parameters for the conditional outcome it may not necessarily lead to an improvement in predicting CATE. This is because  $\text{EIG}_{\theta|\mathcal{D}_0}$  encourages *uniform entropy reduction* across all dimensions of  $\theta$ , not just the ones relevant for CATE estimation. For instance, a dataset of untreated individuals would still provide information about the conditional outcome but much less for the contrast of outcomes required for CATE. This problem motivates our improved methodology given in the next section.

### 3.2 Targeted EIG in CATE Parameters: An Improved Approach to Merge Evaluation

Many causal inference models have additional parameter structure that allows us to more directly target CATE estimation. Specifically, the parameter set,  $\theta$  can be split as  $\theta = \theta_c \cup \theta_{nc}$  where  $\theta_c$  parameterises the CATE model and  $\theta_{nc}$  is a set of nuisance parameters. For example, in Bayesian Causal Forests [23] the model is parameterised as:

$$f_\theta(\mathbf{x}, t) = \mu_{\theta_{nc}}(\mathbf{x}) + t\tau_{\theta_c}(\mathbf{x}),$$

where  $\mu_{\theta_{nc}}, \tau_{\theta_c}(\mathbf{x})$  jointly model the conditional outcome, and  $\tau_{\theta_c}(\mathbf{x})$  directly models CATE. Leveraging such a parameterisation, we can prioritise uncertainty reduction in  $\theta_c$  and therefore CATE by targeting the following:

$$\begin{aligned} \text{EIG}_{\theta_c|\mathcal{D}_0}(e) &= \mathbb{E}_{P(\mathbf{y}_e|\mathbf{X}_e, \mathbf{t}_e, \theta_c)} [H(P(\theta_c|\mathcal{D}_0)) - H(P(\theta_c|\mathcal{D}_0, \mathcal{D}_e))] \\ &= \mathbb{E}_{P(\mathbf{y}_e, \theta_c|\mathbf{X}_e, \mathbf{t}_e, \mathcal{D}_0)} \left[ \log \frac{P(\mathbf{y}_e|\theta_c, \mathbf{X}_e, \mathbf{t}_e, \mathcal{D}_0)}{P(\mathbf{y}_e|\mathbf{X}_e, \mathbf{t}_e, \mathcal{D}_0)} \right]. \end{aligned} \quad (5)$$

Where  $P(\mathbf{y}_e|\theta_c, \mathbf{X}_e, \mathbf{t}_e, \mathcal{D}_0) = \mathbb{E}_{P(\theta_{nc}|\theta_c, \mathcal{D}_0)} [P(\mathbf{y}_e|\theta, \mathbf{X}_e, \mathbf{t}_e)]$  is the Bayesian distribution of the outcomes conditional on  $\theta_c$  and the second line has been rearranged as in (3). The challenge now being that  $P(\mathbf{y}_e|\theta_c, \mathbf{X}_e, \mathbf{t}_e, \mathcal{D}_0)$  is given by integrating out  $\theta_{nc}$ , and so isn't available in closed form. Therefore we use a second nested Monte Carlo estimator to approximate  $P(\mathbf{y}_e|\theta_c, \mathbf{X}_e, \mathbf{t}_e, \mathcal{D}_0)$  in the numerator of Equation (5) in addition to the previous nested Monte Carlo estimator of the posterior predictive likelihood  $P(\mathbf{y}_e|\mathbf{X}_e, \mathbf{t}_e, \mathcal{D}_0)$  used in Equation (4). The estimator of  $\text{EIG}_{\theta_c|\mathcal{D}_0}(e)$  is then given by:

$$\begin{aligned} \widehat{\text{EIG}}_{\theta_c|\mathcal{D}_0}(e) &= \frac{1}{N} \sum_{i=1}^N \log \left( \frac{\widehat{P}(\mathbf{y}_e^{(i)}|\theta_c^{(i)}, \mathbf{X}_e, \mathbf{t}_e, \mathcal{D}_0)}{\widehat{P}(\mathbf{y}_e^{(i)}|\mathbf{X}_e, \mathbf{t}_e, \mathcal{D}_0)} \right) \text{ for } \begin{cases} \theta_c^{(i)} \sim P(\theta_c|\mathcal{D}_0), \\ \mathbf{y}_e^{(i)} \sim P(\mathbf{y}_e|\theta_c, \mathbf{X}_e, \mathbf{t}_e) \end{cases} \quad (6) \\ \widehat{P}(\mathbf{y}_e^{(i)}|\mathbf{X}_e, \mathbf{t}_e, \mathcal{D}_0) &= \frac{1}{M_1} \sum_{j=1}^{M_1} P(\mathbf{y}_e^{(i)}|\theta_j', \mathbf{X}_e, \mathbf{t}_e) \text{ for } \theta_j' \sim P(\theta|\mathcal{D}_0) \\ \widehat{P}(\mathbf{y}_e^{(i)}|\theta_c^{(i)}, \mathbf{X}_e, \mathbf{t}_e, \mathcal{D}_0) &= \frac{1}{M_2} \sum_{k=1}^{M_2} P(\mathbf{y}_e^{(i)}|\theta_{nc}^{(ik)} \cup \theta_c^{(i)}, \mathbf{X}_e, \mathbf{t}_e) \text{ for } \theta_{nc}^{(ik)} \sim P(\theta_{nc}^{(ik)}|\theta_c^{(i)}, \mathcal{D}_0). \end{aligned}$$

This ensures that we prioritise a gain in information in the part of the model directly responsible for CATE. We again provide algorithmic details in Appendix A.1.

### 3.3 Procedure and Model Classes

We now apply both procedures to three popular Bayesian causal inference methods: Bayesian Polynomial Regression, Bayesian Causal Forests [23], and Causal Multi-task Gaussian Processes [2]. We describe the standard predictive method as well as the parameter split used to target CATE.

**Bayesian Polynomial Regression** Due to its ubiquity across numerous fields, we first apply our method to Bayesian Polynomial Regression model. This involves specifying an initial polynomial transformation<sup>3</sup>  $\phi: \mathcal{X} \times \mathcal{T} \rightarrow \mathbb{R}^p$ , a mean  $\mu_0$ , and precision matrix  $\Lambda_0$  to parameterise the prior as:

$$f_\theta(\mathbf{x}, t) = \phi(\mathbf{x}, t)^\top \theta, \quad \theta \sim \mathcal{N}(\mu_0, \sigma^2 \Lambda_0^{-1}). \quad (7)$$

$\phi$  allows for higher order, or interaction terms. We further assume  $\phi(\mathbf{x}, t)$  and  $\theta$  can be split as:

$$\phi(\mathbf{x}, t) = [\phi_{nc}(\mathbf{x}) \quad t\phi_c(\mathbf{x})]^\top, \quad \theta = [\theta_{nc} \quad \theta_c]^\top$$

This covers a broad range of Bayesian polynomial regressions, including the selection used in Gelman et al. [22]. Using closed form entropies for Gaussian's the EIG can be derived as:

**Proposition 3.1.** *For the Bayesian Polynomial Regression model defined in Equation (7) we have:*

$$\begin{aligned} \text{EIG}_{\theta|\mathcal{D}_0}(e) &= \log(\det(\phi(\mathbf{X}_e, \mathbf{t}_e)^\top \phi(\mathbf{X}_e, \mathbf{t}_e) + \phi(\mathbf{X}_0, \mathbf{t}_0)^\top \phi(\mathbf{X}_0, \mathbf{t}_0) + \Lambda_0)) + c \\ \text{EIG}_{\theta_c|\mathcal{D}_0}(e) &= \log\left(\det((\mathbf{t}_e \odot \phi_c(\mathbf{X}_e))^\top (\mathbf{t}_e \odot \phi_c(\mathbf{X}_e)) + (\mathbf{t}_0 \odot \phi_c(\mathbf{X}_0))^\top (\mathbf{t}_0 \odot \phi_c(\mathbf{X}_0)) + (\Lambda_0)_{[c,c]})\right) + c' \end{aligned}$$

Where  $c, c'$  are constant in  $e$ , we apply  $\phi, \phi_c$  row-wise and  $\odot$  denotes element-wise multiplication. The proof can be found in Appendix B.2.1.

Note  $\text{EIG}_{\theta|\mathcal{D}_0}(e)$  is standard and can be found in Sebastiani and Wynn [58], for instance.

<sup>3</sup>This could be an arbitrary non-linear function but we focus on polynomial transformations.

**Bayesian Causal Forest[23]** Bayesian Causal Forests (BCF) are one of the most popular causal inference methods, building upon Bayesian Additive Regression Trees (BART) [13], which are themselves a mainstay in observational causal inference [26]. BART models place a prior over the parameters of a fixed number of decision trees with the regularization provided by the prior ensuring the trees do not overfit. BCF implements a combination of independent BART models with parameterisations chosen to specifically target CATE. For instance, writing:

$$f_{\theta}(\mathbf{x}, t) = \mu_{\theta_{nc}}(\mathbf{x}) + t\tau_{\theta_c}(\mathbf{x}),$$

where  $\mu_{\theta_{nc}}, \tau_{\theta_c}(\mathbf{x})$  are independent BART models. More precise details and alternative parameterisations can be found in Appendix B.1. As the posterior is only available via sampling, we estimate both EIGs using nested Monte Carlo as given in (4) and (6).

**Causal Multi-task Gaussian Processes[2]** Causal multi-task Gaussian Processes (GPs) use a vector-valued Gaussian process [4] to jointly model both conditional outcomes, whilst allowing information to be shared between them. Specifically, they make use of the following model:

$$\mathbf{f} = [f(\mathbf{x}, 0) \quad f(\mathbf{x}, 1)]^{\top}, \text{ where } \mathbf{f} \sim \mathcal{GP}(0, \mathbf{K})$$

for a vector-valued kernel  $\mathbf{K} : \mathcal{X} \times \mathcal{X} \rightarrow \mathbb{R}^{2 \times 2}$ . The outcomes are then modelled by evaluating the relevant portion of the GP. Under this setting CATE is modelled as  $\tilde{\tau} = \mathbf{e}\mathbf{f}$  for  $\mathbf{e} = [-1 \quad 1]$  so that  $\tilde{\tau}$  is also a GP given by  $\tilde{\tau} \sim \mathcal{GP}(0, \mathbf{e}^{\top} \mathbf{K} \mathbf{e})$ . The advantage of causal multi-task GPs is that they allow us to get a closed form posterior for  $\tau$  without having to observe any samples from  $Y(1) - Y(0)$ .

As GPs are inherently non-parametric they do not fit directly into the framework laid out in Sections 3.1 and 3.2. This is not a problem for the predictive case as we can replace  $\theta$  with  $\mathbf{f}$  in (3) and get closed form expressions[28]. However for the causal case this creates challenges as we cannot directly evaluate the expressions in (5) with  $\tilde{\tau}$  in the place of  $\theta_c$ . To resolve this we instead focus on entropy reduction in CATE predictions on the host dataset. We denote this by  $\tilde{\tau}(\mathbf{X}_0)$ , where  $\mathbf{X}_0$  is the host data matrix. The information gains  $e$  denote these by  $\text{EIG}_{\mathbf{f}|\mathcal{D}_0}(e)$  and  $\text{EIG}_{\tilde{\tau}(\mathbf{X}_0)|\mathcal{D}_0}(e)$  respectively. As the following proposition shows, both of these are now available in closed form:

**Proposition 3.2.** *Let  $n_e^{(t)}$  be the number of people receiving treatment  $t$  in dataset  $e$ , then we have that the expected information gains can be written in closed form:*

$$\begin{aligned} \text{EIG}_{\mathbf{f}|\mathcal{D}_0} &= \frac{1}{2} \log(\det(\Sigma_1)) - \frac{1}{2} \left( n_e^{(0)} \log(\sigma_0^2) + n_e^{(1)} \log(\sigma_1^2) \right) \\ \text{EIG}_{\tilde{\tau}(\mathbf{X}_0)|\mathcal{D}_0}(e) &= \frac{1}{2} \log \left( \frac{\det(\Sigma_1) \det(\Sigma_2)}{\det(\Sigma)} \right) \end{aligned}$$

Where  $\Sigma_1, \Sigma_2, \Sigma$  are given alongside the proof in Appendix B.3.

## 4 Privacy

For privacy we make use of *Multi-Party Computation* (MPC) [20]. First introduced by Yao [67], MPC focuses on a setting where  $m$  separate parties wish to compute the value of a function  $f(x_1, \dots, x_m)$  where the  $i^{\text{th}}$  party inputs  $x_i$  and wishes to keep this private. To resolve this, MPC involves the specification of a protocol of message passing between parties which if followed would lead to the computation of  $f$ . In this work, we focus on the *semi-honest* setting, in which all parties follow the specified protocol, but some *corrupt* parties will try to learn as much about their peers inputs in the process. The goal is to devise a protocol which will preserve the privacy of the non-corrupt party’s inputs, up to a given computational budget by the adversary. In our setting this means that any collection of corrupt sites should be unable to learn anything about the other sites data whilst performing the EIG calculation. Multi-party computation differs from *differential privacy* [17], a more traditional form of ML privacy, in that it does not focus on the public release of statistics.

For implementing multi-party computation, we employ the open source library CrypTen [34]. CrypTen builds upon PyTorch [49] allowing for standard tensor operations to be performed in an MPC protocol. For arithmetic operations on floating-point values this is achieved as follows: A float,  $x_F$ , is multiplied by some large scaling factor  $B = 2^L$  and rounded to the nearest integer  $\lfloor x_F \rfloor$ , where  $L$  is the number of precision bits. The integer  $\lfloor x_F \rfloor$  is then associated with its equivalence class  $x \in \mathbb{Z}/Q\mathbb{Z}$  where  $\mathbb{Z}/Q\mathbb{Z}$  is a ring of  $Q$  elements. The value  $x$  can then be shared across all  $m$  parties using Shamir secret sharing [59], in which each party gets access to a share of  $x$  is given

by  $[x]_i \in \mathbb{Z}/Q\mathbb{Z}$  which is generated such that the sum of all shares recovers the original value, so  $x = \sum_{i=1}^m [x]_i \pmod{Q}$ . At any point all parties can combine their shares to decode the output as  $x_F \approx x/B$ . We let  $[x] = \{[x]_i\}_{i=1}^m$  denote the set of all shares corresponding to the secret value  $x$ .

Arithmetic operations building on addition are performed locally, so that for two secret values  $[x], [y]$  each party performs  $[z]_i = [x]_i + [y]_i$  and the result,  $z$  is obtained by all parties summing their share. Multiplication is implemented using Beaver triples [7], logarithms are approximated using householder iterations [29], and reciprocals use Newton-Raphson. We implement log-determinants using Cholesky LDL decompositions, which are preferred to standard Cholesky factorisations as they do not require the use of square roots which would require a further approximation in Crypten. This is possible as we only compute the log determinant of positive semi-definite matrices. This provides all the operations necessary to implement the above EIG calculations in a private manner using multi-party computation. If the goal is to return the EIG statistics to the host for them to view, a small amount of noise must be added to ensure this final step does not leak any statistical information. However if the goal is simply to output the best site, this can be achieved via the exponential protocol [17] ensuring minimal information leakage. Finally, it is important to note that the discretisation required to represent a float in the ring  $\mathbb{Z}/Q\mathbb{Z}$  involves some degree of precision loss. Nevertheless, as we empirically demonstrate in the next section, this leads to minimal depreciation in performance, comparing against differential privacy in the linear case.

## 5 Experiments and results

We experimentally validate our approach on a setting where the host has to rank a number of candidate datasets based on the estimated gain from merging with each site. We evaluate on a selection of synthetic and semi-synthetic benchmark datasets as this allows us to form a ground truth ranking using the provided CATE values. We ultimately compare the implied rankings with the ground truth ranking given by the PEHE performance of models trained on the merged datasets  $\mathcal{D}_0 \cup \mathcal{D}_e$  where the PEHE is estimated with hold out samples from  $P_0(\mathbf{x})$ . This procedure is repeated for each model class, to make sure the same predictor is used to gauge the information gain and give the ground truth ranking, leading to one true ranking per model class. Throughout, we tune any model hyper-parameters on the host site when measuring the information gain as well as re-tuning parameters on each merged dataset when getting the ground truth ranking.

To generate the datasets, we begin with an initial, large dataset  $\mathcal{D}$  from which we subsample the host and candidate sites. We do this by choosing a selection function,  $S_e(\mathbf{x}, t)$ , and using it to subsample a dataset of size  $n_e$ , where  $S_e(\mathbf{x}_i, t_i)$  is the probability of subsampling point  $i$  for dataset  $\mathcal{D}_e$ . Varying the selection functions across sites ensures heterogeneity amongst datasets whilst complying with the independences given by the causal structure in Figure 2. We begin by providing an illustrative example on synthetic data before evaluating on the causal benchmarks, specifically: Lalonde [36] and Infant Health and Development Program, or IHDP [26]. Further details alongside additional results can be found in Appendix under sections C and E respectively.

### 5.1 Illustrative experiment

**Concept** To provide intuition for the contrast between our two proposed methods, namely the standard Bayesian approach based on the full parameter set,  $EIG_\theta$  (3), and dataset acquisition targeting the CATE parameters,  $EIG_{\theta_e}$  (5) we start with a simple example where the host can only choose between two candidate sites. We aim to design these sites so that one corresponds to the "ideal" merge for causal purposes, whilst the other contains similar information to the host site. To do this, we simulate the initial, large dataset  $\mathcal{D}$  as if it were a randomised controlled trial with an equal probability of being treated or untreated, and then subsample the host dataset,  $\mathcal{D}_0$ , using a selection function  $S_0(\mathbf{x}, t)$ . We then generate the two sites termed *twin* and *complementary*, with selection functions  $S_0(\mathbf{x}, t)$  and  $1 - S_0(\mathbf{x}, t)$  respectively. We denote these datasets  $\mathcal{D}_{twin}$  and  $\mathcal{D}_{comp}$ .

The intuition behind this choice is that the twin dataset is drawn from the same distribution as the host, but the complementary is drawn from a distribution that causally "complements" the host. By this we mean that if all datasets were the same size, merging  $\mathcal{D}_0$  with the  $\mathcal{D}_{comp}$  would generate a sample from the initial dataset  $\mathcal{D}$ , and so a sample from a randomised control trial. This is because the variable  $e$  serves as a collider for  $\mathbf{x}$  and  $t$ , and so merging deletes the conditional dependency between  $\mathbf{x}$  and  $t$  (see causal DAG in Appendix 4). Therefore,  $\mathcal{D}_{comp}$  should correspond to an ideal merge as it balances treatment allocation. This is in contrast to  $\mathcal{D}_{twin}$  which provides more information about

similar regions of the data space to those already present in the host,  $\mathcal{D}_0$ , potentially amplifying pre-existing biases and imbalances.

For the illustrative experiment, we vary the ratio of sample sizes,  $\frac{n_{twin}}{n_{comp}}$ , in order to compare which dataset is chosen by  $EIG_{\theta|\mathcal{D}_0}$  and the causally targeted  $EIG_{\theta_c|\mathcal{D}_0}$  for linear regression. The aim is to demonstrate that  $EIG_{\theta|\mathcal{D}_0}$  will preference  $\mathcal{D}_{twin}$  at points where  $\mathcal{D}_{comp}$  dataset is still the preferable dataset for CATE estimation. Indeed, for large values of the ratio  $\frac{n_{twin}}{n_{comp}}$ ,  $\mathcal{D}_{twin}$  provides significant information about the conditional outcome, but not in the regions that are most relevant for causal estimation. On the other hand,  $EIG_{\theta_c}$  should continue to select  $\mathcal{D}_{twin}$  whilst it remains preferable for CATE estimation. We simulate  $\mathbf{x} \in \mathbb{R}^3$  where  $x_1$  is Bernoulli and other covariates are normal. The true outcome is sampled from a normal linear model, and the selection functions are logistic regressions. We also include sample based estimates for each EIG to demonstrate how a closed form method differs from its sample based counterpart. Experimental details provided in Appendix C.

**Results** Figure 3 shows the results of the experiment divided into three regions. In region one, both methods choose the complementary dataset over the twin dataset which is consistent with ground truth ranking given by the PEHE upon merging. In region two,  $EIG_{\theta|\mathcal{D}_0}$  chooses  $\mathcal{D}_{twin}$  whilst  $EIG_{\theta_c|\mathcal{D}_0}$  opts for  $\mathcal{D}_{comp}$ . Here, the complementary dataset is still the optimal in terms of CATE, but  $EIG_{\theta|\mathcal{D}_0}$  preferences  $\mathcal{D}_{twin}$  as it leads to a greater entropy reduction in the full set of parameters. This result shows that by focusing on the causal parameters alone,  $EIG_{\theta_c|\mathcal{D}_0}$  is able to make the correct decision in selecting  $\mathcal{D}_{comp}$ . In the final region we see all lines have crossed the  $x$  axis, showing that all methods agree with the ground truth in choosing  $\mathcal{D}_{twin}$ . Finally, note that the MCMC estimates broadly agree with the closed form counterparts, with increased variability due to sampling.

## 5.2 Ranking experiment

**Concept** For our main experiment we validate our framework in a setting where the host must choose between numerous potential candidates, each with different distributions. To do so we begin with a standard causal inference benchmark dataset,  $\mathcal{D}$ , and form the host and candidates datasets using subsampling functions,  $S_c(\mathbf{x}, t)$  as detailed above where subsampling function is a logistic regression with random parameters. This ensures that each site has a different covariate distribution. We apply the three methods described in Section 3.3 to estimate

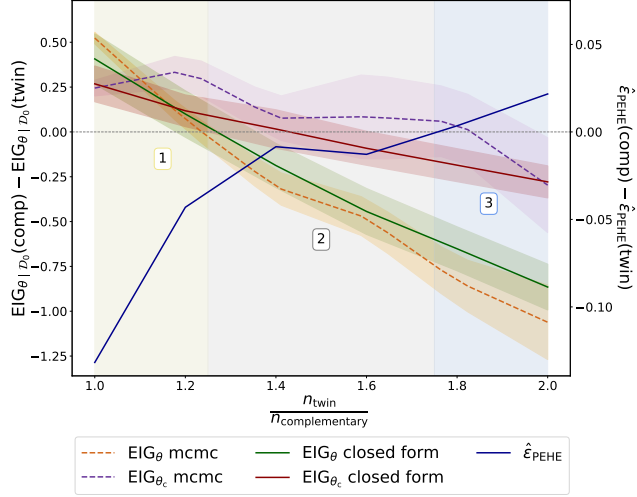


Figure 3: Difference in post host EIG and  $\hat{e}_{PEHE}$  for a linear CATE model trained on  $\mathcal{D}_0 \cup \mathcal{D}_{comp}$  and  $\mathcal{D}_0 \cup \mathcal{D}_{twin}$  for increasing  $\frac{n_{twin}}{n_{comp}}$  and constant  $n_{host} = n_{comp} = 100$ . PEHE is evaluated on hold out data from the host distribution. The plot shows mean  $\pm$  1s.d. cross 50 seeds. The three regions indicate where different datasets are preferred. In region 2,  $EIG_{\theta|\mathcal{D}_0}$  selects  $\mathcal{D}_{twin}$  when  $\mathcal{D}_{twin}$  is the better merge for the causal problem.  $EIG_{\theta_c|\mathcal{D}_0}$  does not share this problem.

Table 1: Results of the ranking experiment for the IHDP dataset measured by Spearman  $\rho$  and precision at k ( $p@k$ ).

	$\rho(\uparrow)$	$p@1(\uparrow)$	$p@3(\uparrow)$	$p@5(\uparrow)$
<b>Polynomial</b>				
$EIG_{\theta \mathcal{D}_0}$	0.70 $\pm$ 0.08	0.50 $\pm$ 0.15	0.70 $\pm$ 0.04	0.78 $\pm$ 0.04
$EIG_{\theta_c \mathcal{D}_0}$	0.68 $\pm$ 0.06	0.50 $\pm$ 0.15	0.70 $\pm$ 0.06	0.76 $\pm$ 0.04
PropScore Error	0.40 $\pm$ 0.11	0.40 $\pm$ 0.15	0.60 $\pm$ 0.15	0.66 $\pm$ 0.04
<b>Causal GP</b>				
$EIG_{\tau(X_0) \mathcal{D}_0}$	0.49 $\pm$ 0.06	0.50 $\pm$ 0.15	0.50 $\pm$ 0.08	0.62 $\pm$ 0.06
$EIG_{f \mathcal{D}_0}$	0.33 $\pm$ 0.06	0.30 $\pm$ 0.15	0.43 $\pm$ 0.05	0.60 $\pm$ 0.04
Sample Size	0.31 $\pm$ 0.12	0.10 $\pm$ 0.20	0.20 $\pm$ 0.07	0.46 $\pm$ 0.05
<b>Bayesian CF</b>				
$EIG_{\theta_c \mathcal{D}_0}$	0.54 $\pm$ 0.10	0.60 $\pm$ 0.15	0.63 $\pm$ 0.08	0.70 $\pm$ 0.04
$EIG_{\theta \mathcal{D}_0}$	0.36 $\pm$ 0.10	0.30 $\pm$ 0.14	0.50 $\pm$ 0.07	0.66 $\pm$ 0.05
PropScore Error	0.45 $\pm$ 0.11	0.60 $\pm$ 0.14	0.63 $\pm$ 0.08	0.70 $\pm$ 0.04

both the two expected information gains for each candidate site,  $\mathcal{D}_e$ . Ultimately, like before, we compare the implied rankings with the ground truth ranking given by the PEHE. Full details are provided in Appendix C.

**Baselines** We provide a number of simple comparison methods as baselines for our task. Specifically, (a) ranking by sample size, (b) ranking by similarity of covariate distribution measured by a multivariate Gaussian fit to the host, and (c) ranking by dissimilarity of treatment allocation measured by the error of a propensity model fit on the host. We compare against baselines via Spearman rho( $\rho$ ) and precision at  $k$  ( $p@k$ ).

**Results** Table 1 shows the results of our experiment on the IHDP dataset[42] where the host has to rank the best datasets out of 10 candidates. We report the average performance of the rankings across 20 repeated experiments, and according to Spearman  $\rho$  [61] and precision at  $k$ . We include the best baseline by Spearman  $\rho$  performance. Additional metrics and the performance of all baselines can be found in the Appendix E. These results demonstrate that across all models, our  $EIG_\theta$  based approach which focuses on causal parameters outperforms the standard approach which seeks expected entropy reduction in all parameters. Results also show that our method works significantly better than all baselines.

### 5.3 Multi-Party Computation Experiments

Finally, we experimentally demonstrate the performance of our cryptographic protocol. We repeat a similar experiment as in Section 5.2 on the IHDP dataset, this time choosing between twenty datasets. Results are given using a linear model as this allows us to compare our MPC based approach against differential privacy<sup>4</sup> (DP) [17] with  $\epsilon = 100$  which is achieved via Laplace noising [18], similar to existing work on DP linear regression [6, 8]. In order to ensure a fair comparison, we noise the final statistics from the MPC computation with an appropriate amount of Laplace noise. This comes from the sensitivity of the EIG statistic which we derive in Appendix A.3. Table 2 shows both the MSE induced by the privacy method and the Spearman  $\rho$  for the deviation from the noise free ranking. Results show that MPC vastly outperforms differential privacy, both in terms of MSE and ranking with DP producing a near random ranking, even with very relaxed noising.

Table 2: Multi-Party Computation Results.

Method	MSE ( $\downarrow$ )	$\rho$ ( $\uparrow$ )
<b>MPC Linear</b> EIG $_{\theta_e}$	$(3.80 \pm 0.04) \times 10^{-6}$	<b>0.797 <math>\pm</math> 0.06</b>
<b>DP Linear</b> EIG $_{\theta_e}$	9.80 $\pm$ 0.30	0.06 $\pm$ 0.11

## 6 Related work

**Federated Learning Via Multi-Party Computation** Our setting bears large with federated learning [38], a distributed machine learning approach that enables multiple parties to collaboratively train a shared model while keeping their raw data decentralised and private. Our goal differs from this as we focus not on learning a model across sites, but deciding which sites to pool. The application of multiparty computation within federated learning is a growing area [32, 39, 47], with much of the work focusing on how to learn predictive models in a secure cross site fashion. Most similar to our work is Muazu et al. [46] who develop a similar federated approach to data fusion focusing on healthcare, however they do not take a causal approach. To the best of our knowledge, there are no existing applications of multi-party computation to problems within causal inference.

**Federated/Private Causal Estimation** There are, however, federated approaches to estimating causal effects. In this area, a majority of works partition the loss function into multiple components, with each component corresponding to a specific data source [41, 64, 65]. However, modelling complex, non-linear relationships remains challenging [3]. Many of these algorithms come without privacy guarantees, with the exception of Niu et al. [48] who add differential privacy (DP) guarantees to various popular CATE estimation techniques. The latter approach however contrasts with ours as the use of sample splitting reduces data efficiency.

**Causal Bayesian Active Learning** Bayesian Active Learning by Disagreement (BALD) [28] is a framework for strategic training data acquisition, focusing on regions of high uncertainty. The  $EIG_{\theta|\mathcal{D}_0}$  method for entropy reduction in all parameters can be viewed as applying BALD after an initial update with datasets instead of datapoints. Most similar to our work in this space is CausalBALD [30], which applies an active learning approach to CATE estimation. However

<sup>4</sup>Definition of differential privacy and its parameters is given in Appendix A.2.

the acquisition function cannot easily be extended to datasets without ignoring the correlation in information provided by different points. Most applications of active learning in causality focus on causal discovery and/or active intervention selection [5, 24, 63].

## 7 Discussion

**Limitations** Due to the cost of computing high dimensional determinants and performing multiple rounds of conditional sampling, our method can be computationally costly in high dimensions. Moreover, the cost of multi-party computation will also increase as higher order approximations are required to retain accuracy. However, both of these remain negligible compared to the data engineering and expenses of data fusion [10, 31]. Finally, whilst our method offers a secure and principled way to prospectively quantify the value of dataset merges, the amount of information needed to justify such expenses may vary depending on application. It might, therefore, be beneficial to consider introducing a problem-specific threshold to determine when a proposed merger is worthwhile.

**Conclusion** We introduce an information-theoretic, cryptographically secure framework for evaluating the utility of potential data merges for causal estimation. To the best of our knowledge, this is the first work addressing this relevant challenge. Through empirical evaluation, we demonstrate that our framework can reliably rank datasets according to their ability to improve CATE estimation. We show that entropy reduction in the CATE parameters alone gives an improvement when compared to a more standard approach to Bayesian dataset acquisition. Finally, we demonstrate that our cryptographic procedure can be applied with minimal loss of accuracy, vastly outperforming differentially privacy.

## Acknowledgements

We thank the reviewers for their constructive feedback. We would like to thank Andrew Yiu, Amartya Sanyal, Shahine Bouhabid, Xi Lin and Sahra Ghalebikesabi for their help.

## References

- [1] K. Abouelmehdi, A. Beni-Hessane, and H. Khaloufi. Big healthcare data: preserving security and privacy. *Journal of big data*, 5(1):1–18, 2018. 1
- [2] A. M. Alaa and M. Van Der Schaar. Bayesian inference of individualized treatment effects using multi-task gaussian processes. *Advances in neural information processing systems*, 30, 2017. 2, 5, 6, 18
- [3] A. Almodóvar, J. Parras, and S. Zazo. Federated learning for causal inference using deep generative disentangled models. In *Deep Generative Models for Health Workshop NeurIPS 2023*, 2023. 9, 21, 22
- [4] M. A. Alvarez, L. Rosasco, N. D. Lawrence, et al. Kernels for vector-valued functions: A review. *Foundations and Trends® in Machine Learning*, 4(3):195–266, 2012. 6, 18
- [5] Y. Annadani, P. Tigas, D. R. Ivanova, A. Jesson, Y. Gal, A. Foster, and S. Bauer. Differentiable multi-target causal bayesian experimental design. *arXiv preprint arXiv:2302.10607*, 2023. 10
- [6] J. Awan and A. Slavković. Structure and sensitivity in differential privacy: Comparing k-norm mechanisms. *Journal of the American Statistical Association*, 116(534):935–954, 2021. 9
- [7] D. Beaver. Efficient multiparty protocols using circuit randomization. In *Advances in Cryptology—CRYPTO’91: Proceedings 11*, pages 420–432. Springer, 1992. 7
- [8] G. Bernstein and D. R. Sheldon. Differentially private bayesian linear regression. *Advances in Neural Information Processing Systems*, 32, 2019. 9
- [9] E. V. Bonilla, K. Chai, and C. Williams. Multi-task gaussian process prediction. *Advances in neural information processing systems*, 20, 2007. 18
- [10] M. L. Brodie. Data integration at scale: From relational data integration to information ecosystems. In *2010 24th IEEE International Conference on Advanced Information Networking and Applications*, pages 2–3. IEEE, 2010. 10
- [11] F. Castanedo et al. A review of data fusion techniques. *The scientific world journal*, 2013, 2013. 1
- [12] K. Chaloner and I. Verdinelli. Bayesian experimental design: A review. *Statistical science*, pages 273–304, 1995. 2, 4
- [13] H. A. Chipman, E. I. George, and R. E. McCulloch. Bart: Bayesian additive regression trees. *Annals of Applied Statistics*, 6(1):266–298, 2012. 6, 16
- [14] R. K. Crump, V. J. Hotz, G. W. Imbens, and O. A. Mitnik. Dealing with limited overlap in estimation of average treatment effects. *Biometrika*, 96(1):187–199, 2009. 2
- [15] R. H. Dehejia and S. Wahba. Causal effects in nonexperimental studies: Reevaluating the evaluation of training programs. *Journal of the American statistical Association*, 94(448):1053–1062, 1999. 21
- [16] A. Doan, A. Halevy, and Z. Ives. *Principles of data integration*. Elsevier, 2012. 1
- [17] C. Dwork. Differential privacy. In *International colloquium on automata, languages, and programming*, pages 1–12. Springer, 2006. 2, 6, 7, 9
- [18] C. Dwork, A. Roth, et al. The algorithmic foundations of differential privacy. *Foundations and Trends® in Theoretical Computer Science*, 9(3–4):211–407, 2014. 9
- [19] European Commission. Data protection rules for the public sector. Retrieved from [https://ec.europa.eu/info/law/law-topic/data-protection/reform/rules-public-sector\\_en](https://ec.europa.eu/info/law/law-topic/data-protection/reform/rules-public-sector_en), 2018. 1
- [20] D. Evans, V. Kolesnikov, M. Rosulek, et al. A pragmatic introduction to secure multi-party computation. *Foundations and Trends® in Privacy and Security*, 2(2-3):70–246, 2018. 2, 6

- [21] A. E. Foster. *Variational, Monte Carlo and policy-based approaches to Bayesian experimental design*. PhD thesis, University of Oxford, 2021. 4
- [22] A. Gelman, J. Hill, and A. Vehtari. *Regression and other stories*. Cambridge University Press, 2021. 2, 5
- [23] P. R. Hahn, J. S. Murray, and C. M. Carvalho. Bayesian regression tree models for causal inference: Regularization, confounding, and heterogeneous effects (with discussion). *Bayesian Analysis*, 15(3):965–1056, 2020. 2, 5, 6, 17
- [24] A. Hauser and P. Bühlmann. Two optimal strategies for active learning of causal models from interventional data. *International Journal of Approximate Reasoning*, 55(4):926–939, 2014. 10
- [25] J. He, S. Yalov, and P. R. Hahn. Xbart: Accelerated bayesian additive regression trees. In *The 22nd International Conference on Artificial Intelligence and Statistics*, pages 1130–1138. PMLR, 2019. 17
- [26] J. L. Hill. Bayesian nonparametric modeling for causal inference. *Journal of Computational and Graphical Statistics*, 20(1):217–240, 2011. 3, 6, 7, 20
- [27] P. W. Holland. Statistics and causal inference. *Journal of the American statistical Association*, 81(396):945–960, 1986. 2
- [28] N. Houlsby, F. Huszár, Z. Ghahramani, and M. Lengyel. Bayesian active learning for classification and preference learning. *arXiv preprint arXiv:1112.5745*, 2011. 4, 6, 9, 22
- [29] A. S. Householder. The numerical treatment of a single nonlinear equation. (*No Title*), 1970. 7
- [30] A. Jesson, P. Tigas, J. van Amersfoort, A. Kirsch, U. Shalit, and Y. Gal. Causal-bald: Deep bayesian active learning of outcomes to infer treatment-effects from observational data. *Advances in Neural Information Processing Systems*, 34:30465–30478, 2021. 9, 22
- [31] A. Kadadi, R. Agrawal, C. Nyamful, and R. Atiq. Challenges of data integration and interoperability in big data. In *2014 IEEE international conference on big data (big data)*, pages 38–40. IEEE, 2014. 10
- [32] R. Kanagavelu, Z. Li, J. Samsudin, Y. Yang, F. Yang, R. S. M. Goh, M. Cheah, P. Wiwatphonthana, K. Akkarajitsakul, and S. Wang. Two-phase multi-party computation enabled privacy-preserving federated learning. In *2020 20th IEEE/ACM International Symposium on Cluster, Cloud and Internet Computing (CCGRID)*, pages 410–419. IEEE, 2020. 9
- [33] A. Kirsch, J. Van Amersfoort, and Y. Gal. Batchbald: Efficient and diverse batch acquisition for deep bayesian active learning. *Advances in neural information processing systems*, 32, 2019. 2
- [34] B. Knott, S. Venkataraman, A. Hannun, S. Sengupta, M. Ibrahim, and L. van der Maaten. Crypten: Secure multi-party computation meets machine learning. *Advances in Neural Information Processing Systems*, 34:4961–4973, 2021. 2, 6
- [35] N. Krantsevich, J. He, and P. R. Hahn. Stochastic tree ensembles for estimating heterogeneous effects. In *International Conference on Artificial Intelligence and Statistics*, pages 6120–6131. PMLR, 2023. 17
- [36] R. J. LaLonde. Evaluating the econometric evaluations of training programs with experimental data. *The American economic review*, pages 604–620, 1986. 7, 20
- [37] M. Lenzerini. Data integration: A theoretical perspective. In *Proceedings of the twenty-first ACM SIGMOD-SIGACT-SIGART symposium on Principles of database systems*, pages 233–246, 2002. 1
- [38] L. Li, Y. Fan, M. Tse, and K.-Y. Lin. A review of applications in federated learning. *Computers & Industrial Engineering*, 149:106854, 2020. 9
- [39] Y. Li, Y. Zhou, A. Jolfaei, D. Yu, G. Xu, and X. Zheng. Privacy-preserving federated learning framework based on chained secure multiparty computing. *IEEE Internet of Things Journal*, 8(8):6178–6186, 2020. 9

- [40] D. V. Lindley. On a measure of the information provided by an experiment. *The Annals of Mathematical Statistics*, 27(4):986–1005, 1956. 2, 4
- [41] Y. Liu, H. Wang, S. Wang, Z. He, W. Xu, J. Zhu, and F. Yang. Disentangle estimation of causal effects from cross-silo data. *arXiv preprint arXiv:2401.02154*, 2024. 9, 21
- [42] C. Louizos, U. Shalit, J. M. Mooij, D. Sontag, R. Zemel, and M. Welling. Causal effect inference with deep latent-variable models. *Advances in neural information processing systems*, 30, 2017. 9
- [43] D. J. MacKay. Information-based objective functions for active data selection. *Neural computation*, 4(4):590–604, 1992. 2
- [44] B. McMahan, E. Moore, D. Ramage, S. Hampson, and B. A. y Arcas. Communication-efficient learning of deep networks from decentralized data. In *Artificial intelligence and statistics*, pages 1273–1282. PMLR, 2017. 21
- [45] M. M. Mello, J. K. Francer, M. Wilenzick, P. Teden, B. E. Bierer, and M. Barnes. Preparing for responsible sharing of clinical trial data, 2013. 1
- [46] T. Muazu, Y. Mao, A. U. Muhammad, M. Ibrahim, U. M. M. Kumshe, and O. Samuel. A federated learning system with data fusion for healthcare using multi-party computation and additive secret sharing. *Computer Communications*, 216:168–182, 2024. 9
- [47] V. Mugunthan, A. Polychroniadou, D. Byrd, and T. H. Balch. Smpai: Secure multi-party computation for federated learning. In *Proceedings of the NeurIPS 2019 Workshop on Robust AI in Financial Services*, volume 21. MIT Press Cambridge, MA, USA, 2019. 9
- [48] F. Niu, H. Nori, B. Quistorff, R. Caruana, D. Ngwe, and A. Kannan. Differentially private estimation of heterogeneous causal effects. In *Conference on Causal Learning and Reasoning*, pages 618–633. PMLR, 2022. 9, 22
- [49] A. Paszke, S. Gross, F. Massa, A. Lerer, J. Bradbury, G. Chanan, T. Killeen, Z. Lin, N. Gimelshein, L. Antiga, et al. Pytorch: An imperative style, high-performance deep learning library. *Advances in neural information processing systems*, 32, 2019. 6
- [50] J. Pearl. Causal inference in statistics: An overview. 2009. 3
- [51] J. Platt and S. Kardia. Public trust in health information sharing: implications for biobanking and electronic health record systems. *Journal of personalized medicine*, 5(1):3–21, 2015. 1
- [52] T. Rainforth, R. Cornish, H. Yang, A. Warrington, and F. Wood. On nesting monte carlo estimators. In *International Conference on Machine Learning*, pages 4267–4276. PMLR, 2018. 4
- [53] T. Rainforth, A. Foster, D. R. Ivanova, and F. Bickford Smith. Modern bayesian experimental design. *Statistical Science*, 39(1):100–114, 2024. 2, 4
- [54] T. S. Richardson and J. M. Robins. Single world intervention graphs (swigs): A unification of the counterfactual and graphical approaches to causality. *Center for the Statistics and the Social Sciences, University of Washington Series. Working Paper*, 128(30):2013, 2013. 3
- [55] D. B. Rubin. Estimating causal effects of treatments in randomized and nonrandomized studies. *Journal of Educational Psychology*, 66(5):688–701, 1974. 3
- [56] D. B. Rubin. Estimating causal effects from large data sets using propensity scores. *Annals of internal medicine*, 127(8\_Part\_2):757–763, 1997. 2
- [57] F. Sattler, S. Wiedemann, K.-R. Müller, and W. Samek. Robust and communication-efficient federated learning from non-iid data. *IEEE transactions on neural networks and learning systems*, 31(9):3400–3413, 2019. 21
- [58] P. Sebastiani and H. P. Wynn. Maximum entropy sampling and optimal bayesian experimental design. *Journal of the Royal Statistical Society: Series B (Statistical Methodology)*, 62(1): 145–157, 2000. 4, 5

- [59] A. Shamir. How to share a secret. *Communications of the ACM*, 22(11):612–613, 1979. 6
- [60] R. Shokri and V. Shmatikov. Privacy-preserving deep learning. In *Proceedings of the 22nd ACM SIGSAC conference on computer and communications security*, pages 1310–1321, 2015. 21
- [61] C. Spearman. The proof and measurement of association between two things. 1961. 9
- [62] S. Tarumi, M. Suzuki, H. Yoshida, S. Miyauchi, and R. Kurazume. Personalized federated learning for institutional prediction model using electronic health records: A covariate adjustment approach. In *2023 45th Annual International Conference of the IEEE Engineering in Medicine & Biology Society (EMBC)*, pages 1–4. IEEE, 2023. 22
- [63] C. Toth, L. Lorch, C. Knoll, A. Krause, F. Pernkopf, R. Peharz, and J. Von Kügelgen. Active bayesian causal inference. *Advances in Neural Information Processing Systems*, 35:16261–16275, 2022. 10
- [64] T. V. Vo, A. Bhattacharyya, Y. Lee, and T.-Y. Leong. An adaptive kernel approach to federated learning of heterogeneous causal effects. *Advances in Neural Information Processing Systems*, 35:24459–24473, 2022. 9, 21, 22
- [65] T. V. Vo, T.-Y. Leong, et al. Federated learning of causal effects from incomplete observational data. *arXiv preprint arXiv:2308.13047*, 2023. 9, 22
- [66] H. Wang, Z. Kaplan, D. Niu, and B. Li. Optimizing federated learning on non-iid data with reinforcement learning. In *IEEE INFOCOM 2020-IEEE conference on computer communications*, pages 1698–1707. IEEE, 2020. 21
- [67] A. C. Yao. Protocols for secure computations. In *23rd annual symposium on foundations of computer science (sfcs 1982)*, pages 160–164. IEEE, 1982. 2, 6

## A Mathematical Details

### A.1 Algorithms for Computing EIG

In this section we provide algorithmic forms of the nested EIG calculations.

---

**Algorithm 1** Algorithm for  $\widehat{\text{EIG}}_{\theta|\mathcal{D}_0}^{\text{NMC}}(e)$

---

**Input:** Data Matrix  $\mathbf{X}_e$ , Treatment Vector  $\mathbf{t}_e$ , Variance  $\sigma^2$   
**Output:**  $\widehat{\text{EIG}}_{\theta|\mathcal{D}_0}^{\text{NMC}}(e)$   
**Require:**  $l = NM_1$  for some  $n, M_1 > 0$   
 $S \leftarrow 0$   
 Sample  $\{\theta_i\}_{i=1}^l \sim P(\theta | \mathcal{D}_0)$  for  $l = NM_1$   
 Split  $\{\theta_i\}_{i=1}^l$  as  $\{(\theta_i), (\theta_{i,j})_{j=1}^{M_1}\}_{i=1}^N$   
**for**  $i \in \{1, \dots, N\}$  **do**  
   Sample  $\mathbf{y}_e^{(i)} \sim P(\mathbf{y}_e | \mathbf{X}_e, \mathbf{t}_e, \theta_i)$   
    $S \leftarrow S + \log \frac{P(\mathbf{y}_e^{(i)} | \theta_i, \mathbf{X}_e, \mathbf{t}_e)}{\frac{1}{M_1} \sum_{j=1}^{M_1} P(\mathbf{y}_e^{(i)} | \theta_{i,j}, \mathbf{X}_e, \mathbf{t}_e)}$   
**end for**  
 $\widehat{\text{EIG}}_{\theta|\mathcal{D}_0}^{\text{NMC}}(e) \leftarrow \frac{1}{N} S$   
**return**  $\widehat{\text{EIG}}_{\theta|\mathcal{D}_0}^{\text{NMC}}(e)$

---



---

**Algorithm 2** Algorithm for  $\widehat{\text{EIG}}_{\theta|\mathcal{D}_0}^{\text{RB}}(e)$

---

**Input:**  $\{\theta_i\}_{i=1}^l \sim P(\theta | \mathcal{D}_0)$ , Data Matrix  $\mathbf{X}_e$ , Treatment Vector  $\mathbf{t}_e$ , Variance  $\sigma^2$   
**Output:**  $\widehat{\text{EIG}}_{\theta|\mathcal{D}_0}^{\text{RB}}(e)$   
 $S \leftarrow 0$   
 Sample  $\{\theta_i\}_{i=1}^l \sim P(\theta | \mathcal{D}_0)$  for  $l = NM_1$   
 Split  $\{\theta_i\}_{i=1}^l$  as  $\{(\theta_i), (\theta_{i,j})_{j=1}^{M_1}\}_{i=1}^N$   
**for**  $i \in \{1, \dots, N\}$  **do**  
   Sample  $\mathbf{y}_e^{(i)} \sim P(\mathbf{y}_e | \mathbf{X}_e, \mathbf{t}_e, \theta_i)$   
    $S \leftarrow S - \log \frac{1}{M_1} \sum_{j=1}^{M_1} P(\mathbf{y}_e^{(i)} | \theta_{i,j}, \mathbf{X}_e, \mathbf{t}_e)$   
**end for**  
 $\widehat{\text{EIG}}_{\theta|\mathcal{D}_0}^{\text{RB}}(e) \leftarrow \frac{1}{N} S$   
**return**  $\widehat{\text{EIG}}_{\theta|\mathcal{D}_0}^{\text{NMC}}(e)$

---

### A.2 Differential Privacy Definition

**Definition A.1.** We say a randomised algorithm,  $\mathcal{A}$  satisfies  $\epsilon$  differential privacy if for any input dataset  $\mathcal{D}$  and dataset  $\mathcal{D}'$  differing by a single entry, we have

$$P(\mathcal{A}(\mathcal{D}) \in \mathcal{O}) \leq \exp(\epsilon) P(\mathcal{A}(\mathcal{D}') \in \mathcal{O}).$$

### A.3 Sensitivity of Linear Statistic

We derive the sensitivity of the linear EIG statistic in order to give a fair comparison with naive differential privacy in Section ??.

**Proposition A.1.** Let:

$$f(\mathbf{X}_e) = \log \det(\mathbf{X}_e^\top \mathbf{X}_e + \mathbf{X}_0^\top \mathbf{X}_0 + \Lambda_0) \quad (8)$$

---

**Algorithm 3** Algorithm for  $\widehat{\text{EIG}}_{\theta_c|\mathcal{D}_0}(e)$ 


---

**Input** Data Matrix  $\mathbf{X}_e$ , Treatment Vector  $\mathbf{t}_e$ , Variance  $\sigma^2$   
**Output:**  $\widehat{\text{EIG}}_{\theta_c|\mathcal{D}_0}(e)$   
 $S \leftarrow 0$   
 Sample  $\{\theta_i\}_{i=1}^N \sim P(\theta | \mathcal{D}_0)$   
**for**  $i \in \{1, \dots, N\}$  **do**  
   Sample  $\mathbf{y}_e \sim P(\mathbf{y}_e | \theta, \mathbf{X}_e, \mathbf{t}_e)$   
   Sample  $\{\theta'_j\}_{j=1}^{M_1} \sim P(\theta | \mathcal{D}_0)$   
   Sample  $\{(\theta_{\text{nc}})^{(ik)}\}_{k=1}^{M_2} \sim P(\theta_{\text{nc}} | (\theta_c)_i, \mathcal{D}_0)$   
    $\widehat{P}(\mathbf{y}_e^{(i)} | \mathbf{X}_e, \mathbf{t}_e, \mathcal{D}_0) \leftarrow \frac{1}{M_1} \sum_{j=1}^{M_1} P(\mathbf{y}_e^{(i)} | \theta'_j, \mathbf{X}_e, \mathbf{t}_e)$   
    $\widehat{P}(\mathbf{y}_e^{(i)} | \theta_c^{(i)}, \mathbf{X}_e, \mathbf{t}_e, \mathcal{D}_0) \leftarrow \frac{1}{M_2} \sum_{k=1}^{M_2} P(\mathbf{y}_e^{(i)} | \theta_{\text{nc}}^{(ik)} \cup \theta_c^{(i)}, \mathbf{X}_e, \mathbf{t}_e)$   
    $S \leftarrow S + \log\left(\frac{\widehat{P}(\mathbf{y}_e^{(i)} | \theta_c^{(i)}, \mathbf{X}_e, \mathbf{t}_e, \mathcal{D}_0)}{\widehat{P}(\mathbf{y}_e^{(i)} | \mathbf{X}_e, \mathbf{t}_e, \mathcal{D}_0)}\right)$   
**end for**  
**return**  $\frac{1}{N} S$

---

If  $\Lambda_0 = cI$  and  $\|\mathbf{x}\|_\infty \leq M$  for all  $\mathbf{x} \sim P_e(\mathbf{x})$  and  $e$ . Then we have that:

$$\Delta_f = \max_{\mathbf{X}'_e, \mathbf{X}_e} |f(\mathbf{X}'_e) - f(\mathbf{X}_e)| \leq \frac{Md}{\sqrt{c}} \quad (9)$$

Where  $\mathbf{X}'_e, \mathbf{X}_e$  differ in at most one row. This implies  $f(\mathbf{X}_e) + Z$  for  $Z \sim \text{Laplace}(\frac{Md}{\epsilon\sqrt{c}})$  is a  $\epsilon$  differentially private release of  $f(\mathbf{X}_e)$ .

*Proof.* To prove this we will use the fact that if  $\max_{\|\mathbf{x}\| \leq M} \|Df(\mathbf{x})\|_F = L$  we have that  $|f(\mathbf{X}'_e) - f(\mathbf{X}_e)| \leq L \|\mathbf{X}'_e - \mathbf{X}_e\|_F$  for all  $\mathbf{X}'_e, \mathbf{X}_e$  with norm bounded by  $M$  where  $\|\cdot\|_F$  is the Frobenious norm. Write  $\mathbf{E} = \mathbf{X}_0^\top \mathbf{X}_0 + \Lambda_0$ , via the chain rule we have that  $Df(\mathbf{X}) = (\mathbf{X}_e^\top \mathbf{X}_e + \mathbf{E})^{-1} \mathbf{X}_e^\top$  Now:

$$\|(\mathbf{X}_e^\top \mathbf{X}_e + \mathbf{E})^{-1} \mathbf{X}_e^\top\|_F = \sqrt{\text{tr}\left((\mathbf{X}_e^\top \mathbf{X}_e + \mathbf{E})^{-1} \mathbf{X}_e^\top \mathbf{X}_e (\mathbf{X}_e^\top \mathbf{X}_e + \mathbf{E})^{-1}\right)} \quad (10)$$

$$= \sqrt{\text{tr}\left((\mathbf{X}_e^\top \mathbf{X}_e + \mathbf{E})^{-1} - (\mathbf{X}_e^\top \mathbf{X}_e + \mathbf{E})^{-1} \mathbf{E} (\mathbf{X}_e^\top \mathbf{X}_e + \mathbf{E})^{-1}\right)} \quad (11)$$

$$\leq \sqrt{\text{tr}\left((\mathbf{X}_e^\top \mathbf{X}_e + \mathbf{E})^{-1}\right)} \leq \sqrt{\frac{d}{c}} \quad (12)$$

We have used the fact that  $(\mathbf{X}_e^\top \mathbf{X}_e + \mathbf{E})^{-1} \mathbf{E} (\mathbf{X}_e^\top \mathbf{X}_e + \mathbf{E})^{-1}$  is positive semi definite and so has positive trace, and that the eigenvalues of  $\mathbf{X}_e^\top \mathbf{X}_e + \mathbf{E}$  are bounded below by  $c$  so the eigenvalues of  $(\mathbf{X}_e^\top \mathbf{X}_e + \mathbf{E})^{-1}$  are bounded above by  $\frac{1}{c}$ . Finally for neighbouring datasets we can change at most  $d$  entries by  $M$  so  $\|\mathbf{X}'_e - \mathbf{X}_e\|_F \leq \sqrt{d}M$   $\square$

## B Model Details

Throughout all methods will aim to model the outcome as some function plus an error, so:

$$Y_i = f(\mathbf{x}_i, t_i) + \epsilon_i \quad (13)$$

### B.1 Models via Sampling

**Bayesian Additive Regression Trees (BART)** BART models [13]  $f$  as the sum of  $L$  piecewise constant binary regression trees, so we have:

$$f(\mathbf{x}, t) = \sum_{l=1}^L g_l(\mathbf{x}, t, T_l, \mathbf{m}_l) \quad (14)$$

where  $T_l$  is a regression tree given by a partition  $(\mathcal{A}_1, \dots, \mathcal{A}_{B(l)})$  of  $\mathcal{X} \times \mathcal{T}$  and the set of leaf parameter values  $\mathbf{m}_l = (m_{l1}, \dots, m_{lB(l)})$  so that:

$$g_l(\mathbf{x}, t) = m_j \text{ if } \mathbf{x}, t \in \mathcal{A}_j \quad (15)$$

The mean parameters are given with independent normal parameters  $m_{lj} \sim \mathcal{N}(0, \sigma_m)$ . Over trees, the prior is such that the probability of a node having children at depth  $d$  is given by:

$$\alpha(1+d)^{-\theta} \text{ for } \alpha \in (0, 1), \theta \in [0, \infty) \quad (16)$$

The original BART model explores this space using Metropolis-Hastings Markov chain Monte Carlo, but we make use of XBART [25] for accelerated posterior sampling.

**Bayesian Causal Forest** [23] Bayesian Causal Forests build upon BART models utilising specific parameterisations for causal inference tasks. The two parameterisations suggested in Hanh et al [23] are firstly:

$$f(\mathbf{x}, t) = \mu(\mathbf{x}) + t\tau(\mathbf{x}) \quad (17)$$

Where  $\mu, \tau$  are independent BART models. To draw specific attention to their parameters will write them as  $\mu_{\theta_{nc}}, \tau_{\theta_c}$  noting that  $\tau_{\theta_c}$  is a model for CATE. Hanh et al [23] note that this parameterisation is not invariant to which treatment is assigned as positive or negative, leading them to propose the following invariant parameterisation:

$$f_{\theta}(\mathbf{x}, t) = \tilde{\mu}_{\tilde{\theta}_{nc}}(\mathbf{x}) + b_t \tilde{\tau}_{\tilde{\theta}_c}(\mathbf{x}) \quad (18)$$

Where  $b_t \sim \mathcal{N}(0, \frac{1}{2})$ . Under this parameterisation a CATE estimate is given by  $(b_1 - b_0) \tilde{\tau}_{\tilde{\theta}_c}(\mathbf{x})$ . When sampling we make use of the accelerated Bayesian Causal Forest approach [35] which builds upon XBART and uses the following slightly modified model:

$$f_{\theta}(\mathbf{x}, t) = a \tilde{\mu}_{\tilde{\theta}_{nc}}(\mathbf{x}) + b_t \tilde{\tau}_{\tilde{\theta}_c}(\mathbf{x}) \quad (19)$$

Where  $a \sim \mathcal{N}(0, 1)$ .

We define the set  $\theta_c$  to be any parameters affiliated with the  $\tau$  model, including  $b_t$  for the invariant parameterisation. In order to sample  $P(\theta_{nc} | \theta_c, \mathcal{D}_0)$  we refit  $\theta_{nc}$  parameters on the dataset  $\mathcal{D}_0$  to the residuals resulting from subtracting the  $\tau$  portion of the model. So this refitting  $\mu$  is as follows for the standard parameterisation:

$$Y - t\tau_{\theta_c}(\mathbf{x}) = \mu_{\theta_{nc}}(\mathbf{x}) \quad (20)$$

Or for the accelerated Bayesian Causal Forest approach [35]:

$$Y - b_t \tilde{\tau}_{\tilde{\theta}_c}(\mathbf{x}) = a \tilde{\mu}_{\tilde{\theta}_{nc}}(\mathbf{x}) \quad (21)$$

Where any parameters on the left hand side are fixed.

## B.2 Closed Form Models

In this section we give details of models for which the EIG is available in closed form. We provide details of the models as well as proofs for the expressions.

### B.2.1 Bayesian Polynomial Regression Derivations

In this we derive the results for Bayesian polynomial regression. We have modelled our data as:

$$y \sim \mathcal{N}(\phi(\mathbf{x}, t)^\top \theta, \sigma^2), \quad \theta \sim \mathcal{N}(\mu_0, \sigma^2 \Lambda_0^{-1}) \quad (22)$$

In this context, the posterior is available in closed form as:

$$\theta | \mathcal{D}_0 \sim \mathcal{N}(\mu_0, \sigma^2 \tilde{\Lambda}_0^{-1}) \quad (23)$$

$$\tilde{\Lambda}_0 = \left( \phi(\mathbf{X}_0, \mathbf{t}_0)^\top \phi(\mathbf{X}_0, \mathbf{t}_0) + \Lambda_0^{-1} \right) \quad (24)$$

$$\mu_0 = (\Lambda_0)^{-1} \left( \phi(\mathbf{X}_0, \mathbf{t}_0)^\top \phi(\mathbf{X}_0, \mathbf{t}_0) \hat{\theta}_0 + \Lambda_0 \mu_0 \right) \quad (25)$$

$$\hat{\theta}_0 = \left( \phi(\mathbf{X}_0, \mathbf{t}_0)^\top \phi(\mathbf{X}_0, \mathbf{t}_0) \right)^{-1} \phi(\mathbf{X}_0, \mathbf{t}_0)^\top \mathbf{y}_0 \quad (26)$$

**Expected Information Gain Over all parameters** We use the fact that  $\text{EIG}_{\theta|\mathcal{D}_0}$  can be written as:

$$\text{EIG}_{\theta|\mathcal{D}_0}(e) = \mathbb{E}_{P(\mathbf{y}_e|\mathbf{x}_e, \mathbf{t}_e, \mathcal{D}_0)} [H[P(\theta|\mathcal{D}_0)] - H[P(\theta|\mathcal{D}_0, \mathcal{D}_e)]],$$

As the posterior over  $\theta$  is Gaussian we can directly evaluate these expressions using the closed form entropy for a Gaussian distribution as:

$$H[P(\theta|\mathcal{D}_0)] = \frac{n_e}{2} (1 + \log(2\pi)) + \frac{1}{2} \left( \log \det \left( \tilde{\Lambda}_0^{-1} \right) \right)$$

The distribution  $\theta|\mathcal{D}_0, \mathcal{D}_e$  can be obtained as above, where we now use  $\tilde{\Lambda}_0$  as the prior precision matrix before updating on  $\mathcal{D}_0$ . This gives:

$$H[P(\theta|\mathcal{D}_0)] = \frac{n_e}{2} (1 + \log(2\pi)) + \frac{1}{2} \left( \log \det \left( \left( \phi(\mathbf{X}_e, \mathbf{t}_e)^\top \phi(\mathbf{X}_e, \mathbf{t}_e) + \tilde{\Lambda}_0 \right)^{-1} \right) \right)$$

Using the above form for  $\tilde{\Lambda}_0$  and collecting all constants gives the expression presented in the text.

**EIG $_{\theta_c|\mathcal{D}_0}$ : Expected Information Gain Over all parameters** This follows as above but using the fact that the block form of the matrices to allow us write the covariance precision matrix for the post host posterior over  $\theta_c$  as follows:

$$(\mathbf{t}_0 \odot \phi_c(\mathbf{X}_0))^\top (\mathbf{t}_0 \odot \phi_c(\mathbf{X}_0)) + (\Lambda_0)_{[c,c]}$$

Where  $(\Lambda_0)_{[c,c]}$  corresponds to block of  $\Lambda_0$  with entries after  $[c, c]$  in the row and column.

### B.3 Causal Multitask Gaussian Processes[2]

In this work, CATE is modelled using a multitask Gaussian process [9]. Multitask Gaussian Processes use a GP in vector-valued Reproducing Kernel Hilbert Space (vv-RKHS) to share information between tasks [4]. In Alaa and Van Der Schaar [2] learning the conditional outcome function for each treatment is seen as a separate task, so we jointly model:

$$Y|\mathbf{x}, t \sim \mathcal{N}(0, f_t(\mathbf{x}), \sigma_t^2) \quad (27)$$

Where each  $f_t$  is a Gaussian Process. The kernel  $\mathbf{K}_\eta : \mathcal{X} \times \mathcal{X} \rightarrow \mathbb{R}^{2 \times 2}$  is now a symmetric positive semi-definite matrix-valued function, with hyper-parameters  $\eta$ . In the case of Alaa and Van Der Schaar [2] they use a *linear model of coregionalization*<sup>5</sup>, giving the kernel as:

$$\mathbf{K}_\eta(\mathbf{x}, \mathbf{x}') = \mathbf{A}_0 k_0(\mathbf{x}, \mathbf{x}') + \mathbf{A}_1 k_1(\mathbf{x}, \mathbf{x}') \quad (28)$$

Where  $k_t$  is the RBF kernel, given by:

$$k_t(\mathbf{x}, \mathbf{x}') = \exp\left(-\frac{1}{2} (\mathbf{x} - \mathbf{x}')^\top \mathbf{R}_t^{-1} (\mathbf{x} - \mathbf{x}')\right) \quad (29)$$

Where  $\mathbf{R}_t^{-1} = \text{diag}(\ell_{1,t}^2, \dots, \ell_{d,t}^2)$  and  $\ell_{j,t}$  is the length-scale parameter for the treatment  $T = t$  in the  $j^{\text{th}}$  coordinate of  $\mathbf{x}$ .  $\mathbf{A}_t$  is given by:

$$\mathbf{A}_0 = \begin{bmatrix} \theta_{00}^2 & \rho_0 \\ \rho_0 & \theta_{01}^2 \end{bmatrix}, \mathbf{A}_1 = \begin{bmatrix} \theta_{10}^2 & \rho_1 \\ \rho_1 & \theta_{11}^2 \end{bmatrix}. \quad (30)$$

Where  $\theta_{ij}$  and  $\rho_i$  determine the variances and covariances of the shared tasks  $f_t$ . So we have that the full set of hyper-parameters  $\eta = (\theta_0, \theta_1, \mathbf{R}_0, \mathbf{R}_1, \mathbf{A}_0, \mathbf{A}_1)$ . Once all these hyper-parameters have been learnt we have that the covariance between different function evaluations,  $f_t(\mathbf{x}), f_{t'}(\mathbf{x}')$ , is given the  $t, t'$  coordinate of  $\mathbf{K}_\eta(\mathbf{x}, \mathbf{x}')$ . So:

$$\text{cov}(f_t(\mathbf{x}), f_{t'}(\mathbf{x}')) = \mathbf{K}_\eta(\mathbf{x}, \mathbf{x}')_{[t,t']} \quad (31)$$

Now, if we let  $K((\mathbf{x}, t), (\mathbf{x}', t')) = \mathbf{K}_\eta(\mathbf{x}, \mathbf{x}')_{[t,t']}$  then we can obtain the posterior kernel in a similar way to the standard case. Precisely if we the training data be given by:

$$\tilde{\mathbf{X}} = [\{\mathbf{x}_i\}_{T_i=0}, \{\mathbf{x}_i\}_{T_i=1}]^T, \quad (32)$$

$$\tilde{\mathbf{Y}} = \left[ \left\{ \left\{ y_i^{(T_i)} \right\}_{T_i=0}, \left\{ y_i^{(T_i)} \right\}_{T_i=1} \right\} \right]^T, \quad (33)$$

$$\Sigma = \text{diag}(\sigma_0^2 \mathbf{I}_{n-n_1}, \sigma_1^2 \mathbf{I}_{n_1}) \quad (34)$$

$$n_1 = \sum_i W_i, \quad (35)$$

$$\mathbf{K}_\eta(x) = (\mathbf{K}_\eta(x, X_i))_i \cdot \quad (36)$$

<sup>5</sup>See Alvarez et al. [4] for more details.

Then we have that the posterior multitask GP has mean and posterior kernel given by:

$$m^{\text{post}}(\mathbf{x}) = \mathbf{K}_\eta^T(\mathbf{x}) (\mathbf{K}_\eta(\mathbf{X}, \mathbf{X}) + \Sigma)^{-1} \tilde{\mathbf{Y}} \quad (37)$$

$$\mathbf{K}_{\eta^*}^{\text{post}}(\mathbf{x}, \mathbf{x}') = \mathbf{K}_{\eta^*}(\mathbf{x}, \mathbf{x}') - \mathbf{K}_{\eta^*}(\mathbf{x}) (\mathbf{K}_\eta(\mathbf{X}, \mathbf{X}) + \Sigma)^{-1} \mathbf{K}_{\eta^*}^T(\mathbf{x}') \quad (38)$$

$$(39)$$

This leads to the following posterior over CATE, where  $\mathbf{e} = [-1, 1]^\top$ :

$$\tilde{\tau}(x) \sim \mathcal{N}(m^{\text{post}}(\mathbf{x})^\top \mathbf{e}, \mathbf{e}^\top \mathbf{K}_{\eta^*}^{\text{post}}(\mathbf{x}, \mathbf{x}') \mathbf{e}) \quad (40)$$

### B.3.1 Expected Information Gain

First, let  $\mathbf{X}_e^{(1)}, \mathbf{X}_e^{(0)}$  and  $\mathbf{y}_e^{(1)}, \mathbf{y}_e^{(0)}$  be the covariance and outcomes for environment  $e$  that is treated and untreated respectively. To avoid confusion with treatment we will use  $\mathbf{X}_{e^*}$  to refer to the host environment for this derivation. We will also use  $\mathbf{K}_{|\mathcal{D}_0}$  to refer to the posterior kernel. Now to derive the Expected Information Gain in closed form we need the distribution of the following vector:

$$\begin{bmatrix} \mathbf{y}_e^{(1)} \\ \mathbf{y}_e^{(0)} \\ \tilde{\tau}(\mathbf{X}_{e^*}) \end{bmatrix} | \mathbf{X}_e, \mathcal{D}_0 \sim \mathcal{N}(\mathbf{m}, \Sigma) \quad (41)$$

Where we have that:

$$\Sigma_1 = \begin{bmatrix} \mathbf{K}_{|\mathcal{D}_0}(\mathbf{X}_e^{(0)}, \mathbf{X}_e^{(0)}) + \sigma_0^2 I_{n_e^0} & \mathbf{K}_{|\mathcal{D}_0}(\mathbf{X}_e^{(1)}, \mathbf{X}_e^{(0)}) \\ \mathbf{K}_{|\mathcal{D}_0}(\mathbf{X}_e^{(0)}, \mathbf{X}_e^{(1)}) & \mathbf{K}_{|\mathcal{D}_0}(\mathbf{X}_e^{(1)}, \mathbf{X}_e^{(1)}) + \sigma_1^2 I_{n_e^1} \end{bmatrix} \quad (42)$$

$$\Sigma_2 = \mathbf{K}_{|\mathcal{D}_0}(\mathbf{X}_{e^*}^{(1)}, \mathbf{X}_{e^*}^{(1)}) + \mathbf{K}_{|\mathcal{D}_0}(\mathbf{X}_{e^*}^{(0)}, \mathbf{X}_{e^*}^{(0)}) - 2\mathbf{K}_{|\mathcal{D}_0}(\mathbf{X}_{e^*}^{(1)}, \mathbf{X}_{e^*}^{(0)}) \quad (43)$$

$$\Sigma = \begin{bmatrix} \Sigma_1 & \Sigma_{12} \\ \Sigma_{12}^\top & \Sigma_2 \end{bmatrix} \text{ where } \Sigma_{12} = \begin{bmatrix} \mathbf{K}_{|\mathcal{D}_0}(\mathbf{X}_{e^*}^{(1)}, \mathbf{X}_e^{(0)}) - \mathbf{K}_{|\mathcal{D}_0}(\mathbf{X}_{e^*}^{(0)}, \mathbf{X}_e^{(0)}) \\ \mathbf{K}_{|\mathcal{D}_0}(\mathbf{X}_{e^*}^{(1)}, \mathbf{X}_e^{(1)}) - \mathbf{K}_{|\mathcal{D}_0}(\mathbf{X}_{e^*}^{(0)}, \mathbf{X}_e^{(1)}) \end{bmatrix} \quad (44)$$

Now from the covariance matrix we can derive the standard Expected Information Gain  $\text{EIG}_{\theta|\mathcal{D}_0}$  and CATE-specific  $\text{EIG}_{\theta_c|\mathcal{D}_0}$ . Throughout we will use  $\mathbf{K}$  to the posterior kernel irrespective if it has been fit or not.

**Expected Information Gain over the conditional outcome parameters** For the  $\text{EIG}_f$  we use the BALD form:

$$H(\mathbf{y}_e | \mathbf{X}_e, \mathcal{D}_0) - H(\mathbf{y} | \mathbf{X}_e, \mathbf{f}, \mathcal{D}_0) \quad (45)$$

Using the standard form of entropy for a Gaussian distribution we can read  $H(\mathbf{y}_e | \mathbf{X}_e, \mathcal{D}_0)$  off of the covariance matrix above as:

$$H(\mathbf{y}_e | \mathbf{X}_e, \mathcal{D}_0) = \frac{n_e}{2} (1 + \log(2\pi)) + \frac{1}{2} (\log(|\Sigma_1|)) \quad (46)$$

$$\text{where } \Sigma_1 = \begin{bmatrix} \mathbf{K}_\eta(\mathbf{X}_e^{(0)}, \mathbf{X}_e^{(0)}) + \sigma_0^2 I_{n_e^0} & \mathbf{K}_\eta(\mathbf{X}_e^{(1)}, \mathbf{X}_e^{(0)}) \\ \mathbf{K}_\eta(\mathbf{X}_e^{(0)}, \mathbf{X}_e^{(1)}) & \mathbf{K}_\eta(\mathbf{X}_e^{(1)}, \mathbf{X}_e^{(1)}) + \sigma_1^2 I_{n_e^1} \end{bmatrix} \quad (47)$$

And  $H(\mathbf{y}_e | \mathbf{f}, \mathbf{X}_e, \mathcal{D}_0)$  being:

$$H(\mathbf{y}_e | \mathbf{f}, \mathbf{X}_e, \mathcal{D}_0) = \frac{n_e}{2} (1 + \log(2\pi)) + \frac{1}{2} (n_e^{(0)} \log(\sigma_0^2) + n_e^{(1)} \log(\sigma_1^2)) \quad (48)$$

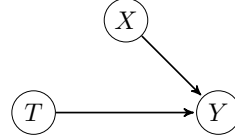
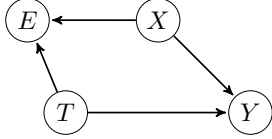
This gives the Expected Information Gain as:

$$\mathcal{I}_f(e) = \frac{1}{2} \log(|\Sigma_1|) - \frac{1}{2} (n_e^{(0)} \log(\sigma_0^2) + n_e^{(1)} \log(\sigma_1^2)) \quad (49)$$

**Expected Information Gain on the CATE parameters** We now target an Expected Information Gain on the CATE parameters on our host dataset, so  $\tilde{\tau}(\mathbf{X}_0)$ . By using the fact that the Expected Information Gain can be written as the mutual information between  $\tilde{\tau}(\mathbf{X}_0)$  and the observed outcomes in dataset  $e$ , we use the closed form mutual information for Gaussian's to directly write this as:

$$\mathcal{I}_{\tilde{\tau}(\mathbf{x}_0)}(e) = \frac{1}{2} \log \left( \frac{|\Sigma_1| |\Sigma_2|}{|\Sigma|} \right) \quad (50)$$

$$\text{where } \Sigma_2 = \mathbf{K}_\eta(\mathbf{X}_{e^*}^{(1)}, \mathbf{X}_{e^*}^{(1)}) + \mathbf{K}_\eta(\mathbf{X}_{e^*}^{(0)}, \mathbf{X}_{e^*}^{(0)}) - 2\mathbf{K}_\eta(\mathbf{X}_{e^*}^{(1)}, \mathbf{X}_{e^*}^{(0)}) \quad (51)$$



(a) Before merging: causal structure in  $D_{host}$ , or  $D_{twin}$  or  $D_{comp}$  taken separately. E acts as a collider and thus creates a dependency between  $X$  and  $T$  (b) After merging: causal structure in  $D_{host} \cup D_{comp}$

Figure 4: Causal structure for the illustrative experiment.

## C Experimental Details

**General experimental settings and hyperparameters** All standard deviations and precisions were taken equal to 1. Throughout experiments, priors were taken as zero-valued vector.

In the **illustrative experiment**, 400 samples were used for computing outer expectations, and 800 samples for inner expectations. Here, we consider  $X = (X_0, X_1, X_2) \in \mathbb{R}^3$ . We use the sampling selection function  $P_{host}(x, t) = \text{sigmoid}(1 + 2 \times x_0 - x_1 + 2 \times t) + \epsilon$  and outcome model  $y = 1 + x_0 - x_1 + x_2 + 5 \times t + 2 \times x_0 + 2 \times x_0 - 4 \times x_2 + \epsilon$  with  $X_0 \sim \mathcal{B}(12, 3)$ ,  $X_1 \sim \mathcal{N}(4, 1)$ ,  $X_2 \sim \mathcal{B}(1, 7)$  and  $\epsilon \sim \mathcal{N}(0, 1)$ .

In both **ranking experiments**, the selection functions are randomly generated. We first generate a binary vector of the size of the dimension of  $X$  to define the subset of covariates that would be impact selection. We then generate two other random vectors, one for the multiplicative coefficients for each selected covariate, and another to define a power for each term in the sum. Ultimately, the probability of selection is taken as the sigmoid of this randomly generated polynomial.

In the **ranking experiment with IHDP**, 10 candidates were generated with a sample size ranging from 300 to 500. The host sample size was equal to 400. The experiment was across 20 seeds. We kept a minimum of 50 subjects in each treatment group. The hold out test dataset had a sample size of 2000. For the linear model,  $X$ ,  $T$  and  $X \times T$  were included. For the Gaussian Process model, a maximum of 1000 iterations was set. In CBF, both the predictive and conditional models were used with a maximum depth of 250, and a shrinkage  $\alpha = 0.95$ .

In the **ranking experiment with Lalonde**, 15 candidates were generated with a sample size ranging from 200 to 400. The host sample size was equal to 600. The experiment was across 20 seeds. We kept a minimum of 50 subjects in each treatment group. The hold out test dataset had a sample size of 2000. For the linear model,  $X$ ,  $T$  and  $X \times T$  were included. For the Gaussian Process model, a maximum of 1000 iterations was set. In CBF, both the predictive and conditional models were used with a maximum depth of 200, and a shrinkage  $\alpha = 0.9$ .

**Datasets** We describe the two datasets used in our experiments, with high-level summary given in Table 3.

Table 3: Description of the datasets: lalonde [36] and IHDP [26].

	ihdp	lalonde
<b>Number of samples</b>	747	16,177
<b>Number of features</b>	24	8

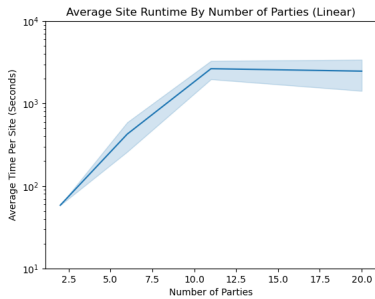
The **Infant Health and Development Program, or IHDP** is a randomized controlled study designed to assess how home visits by specialist doctors impact the cognitive test scores of premature infants. Initially, the dataset serves as a benchmark for evaluating treatment effect estimation algorithms, as described in *Hill et. al* [26]. This evaluation introduces selection bias by excluding non-random subsets of treated individuals to construct an observational dataset, with outcomes derived from the original covariates and treatments.

The **Lalonde** originates from the National Supported Work Demonstration used by *Dehejia and Wahba* [15] to evaluate propensity score matching methods. The data consists of demographic variables (age, race, academic background, and previous real earnings), as well as a treatment indicator. The outcome is the real earnings in the year 1978.

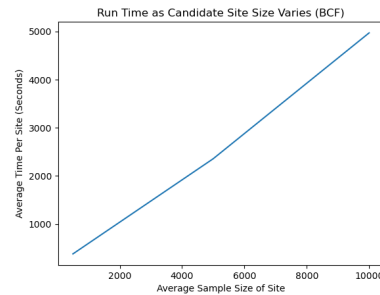
**Compute times** Approximate compute times for the ranking experiment on causal benchmark datasets are given in Table 4. Experiments were performed on an Apple M3 chip with a 12-core CPU and 18 GB of RAM.

Table 4: Approximate compute times.

	<b>ihdp</b>	<b>lalonde</b>
<b>Polynomial</b>	< 1 min	< 1 min
<b>Causal GP</b>	3 mins	3 mins
<b>BART</b>	14 mins	9 mins



(a) In this we repeat the multi-party computation experiments from Section 5.3 varying the number of sites. Each site is treated as a separate party in the multi-party computation and the average runtime per site is reported. Runtime recorded on an M3 macbook. Averaged over 5 runs.



(b) Runtime of Bayesian Causal Forest as the candidate sample size increases. We run the algorithm for the task of selecting between 5 sites with average size 500, 5000, and 10,000.

## D Related work: further details

**On Causal Federated Learning** Federated learning is a distributed machine learning approach that enables multiple parties to collaboratively train a shared model while keeping their raw data decentralised and private. Various federated learning approaches have been proposed, including federated stochastic gradient descent [60], federated averaging [44], and more recently, methods for joint learning of deep neural network models [57, 66]. However, these algorithms do not inherently support causal inference, as the dissimilar distributions across different data sources may lead to biased causal effect estimation. To date, limited research has been conducted on the federated estimation of causal effects, highlighting the need for further exploration in this area. Due to the scope of our work, in the following paragraphs, we will focus on presenting Federated Learning methods for CATE estimation, where covariate distribution and treatment allocation are not assumed to be identical across datasets.

Several methods propose disentangling the loss function to facilitate federated learning. Vo et al. [64] propose CausalRFF, an adaptive kernel approach for causal inference that utilises Random Fourier Features to partition the loss function into multiple components, with each component corresponding to a specific data source. However, CausalRFF approach lacks strong privacy guarantees to prevent data recovery, and modeling complex non-linear relationships remains challenging [3]. Liu et al. [41] introduce a Bayesian method where parameters refer to a local disentangled loss and are updated

cross-silo using server aggregation. Similarly, *Vo et al.* [65] divide the loss function into site-specific functions, and specify a variational posterior distribution for each local loss. Instead of tackling the loss function, Almodóvar et al. [3]) introduce a method based on disentanglement of latent factors into instrumental, confounding, and risk factors, which are then used for treatment effect estimation. They apply federated averaging on a neural network-based generative causal inference model. Ultimately, FedCov [62] is a parametric method for federated adjustment of covariate distributions between sites, where sample weights are derived from a propensity-like model. In all the aforementioned methods, the accuracy of causal estimation is reduced due to the constraints of federated learning. Conversely, our approach does not alter the causal estimation step, thereby maintaining optimal estimation accuracy. The framework we propose focuses on federated learning of the Expected Information Gain that would be obtained by merging with a dataset. While some Federated Causal Learning methods [64, 65] provide uncertainty bounds, which could potentially be used to decide which dataset to merge with by comparing the uncertainty in these bounds, the provided bounds apply to the federated estimate and not the causal estimate potentially obtained after merging. Ultimately, none of these methods provide strong privacy guarantees, such as differential privacy (DP), which would ensure that raw data cannot be recovered from the model parametrization or summary statistics. Moreover, all these methods use the outcome values for training their federated model, and outcome values tend to be more sensitive in nature.

**On Causal Differential Privacy** Contrasting with previous approaches, Niu et al. [48] introduce a meta-algorithm that adds differential privacy (DP) guarantees to various popular CATE estimation frameworks, addressing the privacy concerns mentioned earlier. However, their method relies on multiple sample splitting, where separate subsets of the data are used for estimating the propensity score and the joint response model. This approach allows for parallel composition, a property of differential privacy. In contrast, our work prioritises data efficiency, and aims to utilise the entire dataset for CATE estimation without the need for sample splitting.

**On Bayesian Experimental Design** Bayesian Active Learning by Disagreement (BALD) [28] is a method designed to strategically acquire training data by focusing on regions of high uncertainty. BALD introduces an acquisition function rooted in information theory, which guides the data acquisition process. When reducing entropy towards all parameters in 3.1, we introduce a new setting for BALD where dataset are considered as data points. In the CausalBALD [30] approach, the acquisition function is altered to specifically target areas where the distributions of different treatment groups overlap, thereby maximizing sample efficiency for learning personalised treatment effects. CausalBALD is also made for the acquisition of individual data points. However, contrarily to BALD, CausalBALD’s acquisition function cannot provide a scalar measure if we compute it for a dataset (i.e. a matrix  $\{\mathbf{x}_i, t_i\}_{i=1}^{n_e}$ ) instead of data points (i.e. a vector  $\mathbf{x}_i, t_i$  for a given  $i$ ). To apply CausalBALD in our setting, one would need to approximate the higher-order interaction terms between all combinations of data points within each dataset, thus making the computation intractable.

## E Further experimental results

For completeness, we include the performance of all baselines on the IHDP dataset in Table 5 and the Lalonde in Table 6.

Table 5: IHDP dataset ranking experiment results with 10 candidate datasets

	$\rho(\uparrow)$	$\mathbf{p@1}(\uparrow)$	$\mathbf{p@3}(\uparrow)$	$\mathbf{p@5}(\uparrow)$
<b>Polynomial</b>				
EIG $_{\theta_c \mathcal{D}_0}$	<b>0.70 ± 0.08</b>	<b>0.50 ± 0.15</b>	<b>0.70 ± 0.04</b>	<b>0.78 ± 0.04</b>
EIG $_{\theta \mathcal{D}_0}$	<b>0.68 ± 0.06</b>	<b>0.50 ± 0.15</b>	<b>0.70 ± 0.06</b>	<b>0.76 ± 0.04</b>
PropScore Error	0.40 ± 0.11	0.40 ± 0.15	0.60 ± 0.15	0.66 ± 0.04
Sample Size	0.34 ± 0.08	0.10 ± 0.08	0.27 ± 0.04	0.50 ± 0.06
CovDist	0.03 ± 0.07	0.10 ± 0.08	0.23 ± 0.06	0.48 ± 0.04
<b>Causal GP</b>				
EIG $_{\bar{\tau}(X_0) \mathcal{D}_0}$	<b>0.49 ± 0.06</b>	<b>0.50 ± 0.15</b>	<b>0.50 ± 0.08</b>	<b>0.62 ± 0.06</b>
EIG $_{\mathbf{f} \mathcal{D}_0}$	0.33 ± 0.06	0.30 ± 0.15	0.43 ± 0.05	<b>0.60 ± 0.04</b>
Sample Size	0.31 ± 0.12	0.10 ± 0.20	0.20 ± 0.07	0.46 ± 0.05
PropScore Error	0.21 ± 0.09	0.10 ± 0.20	0.30 ± 0.07	0.43 ± 0.05
CovDist	0.03 ± 0.06	0.10 ± 0.20	0.160 ± 0.04	0.46 ± 0.05
<b>Bayesian CF</b>				
EIG $_{\theta_c \mathcal{D}_0}$	<b>0.54 ± 0.10</b>	<b>0.60 ± 0.15</b>	<b>0.63 ± 0.08</b>	<b>0.70 ± 0.04</b>
EIG $_{\theta \mathcal{D}_0}$	0.36 ± 0.10	0.30 ± 0.14	0.50 ± 0.07	<b>0.66 ± 0.05</b>
PropScore Error	0.45 ± 0.11	<b>0.60 ± 0.14</b>	<b>0.63 ± 0.08</b>	<b>0.70 ± 0.04</b>
Sample Size	0.16 ± 0.09	0.20 ± 0.11	0.26 ± 0.06	0.52 ± 0.05
CovDist	0.07 ± 0.09	0.00 ± 0.00	0.26 ± 0.06 $a$	0.46 ± 0.05

Table 6: Lalonde dataset ranking experiment results with 15 candidate datasets

	$\rho(\uparrow)$	$\mathbf{p@1}(\uparrow)$	$\mathbf{p@3}(\uparrow)$	$\mathbf{p@5}(\uparrow)$
<b>Polynomial</b>				
EIG $_{\theta_c \mathcal{D}_0}$	<b>0.47 ± 0.05</b>	<b>0.40 ± 0.11</b>	<b>0.60 ± 0.05</b>	<b>0.79 ± 0.04</b>
EIG $_{\theta \mathcal{D}_0}$	<b>0.43 ± 0.05</b>	<b>0.35 ± 0.13</b>	0.48 ± 0.04	0.53 ± 0.03
PropScore Error	0.19 ± 0.10	0.20 ± 0.17	0.32 ± 0.06	0.49 ± 0.05
Sample Size	0.24 ± 0.10	0.25 ± 0.08	0.38 ± 0.08	0.58 ± 0.06
CovDist	0.20 ± 0.04	0.25 ± 0.07	0.38 ± 0.06	0.48 ± 0.07
<b>Causal GP</b>				
EIG $_{\bar{\tau}(X_0) \mathcal{D}_0}$	<b>0.42 ± 0.07</b>	<b>0.5 ± 0.12</b>	<b>0.55 ± 0.05</b>	<b>0.72 ± 0.03</b>
EIG $_{\mathbf{f} \mathcal{D}_0}$	<b>0.41 ± 0.04</b>	<b>0.4 ± 0.1</b>	0.43 ± 0.04	0.58 ± 0.07
PropScore Error	0.19 ± 0.05	0.21 ± 0.15	0.32 ± 0.06	0.43 ± 0.07
Sample Size	0.13 ± 0.07	0.15 ± 0.08	0.31 ± 0.09	0.53 ± 0.06
CovDist	0.22 ± 0.04	0.25 ± 0.07	0.36 ± 0.08	0.48 ± 0.04
<b>Bayesian CF</b>				
EIG $_{\theta_c \mathcal{D}_0}$	<b>0.44 ± 0.05</b>	<b>0.45 ± 0.08</b>	<b>0.55 ± 0.05</b>	<b>0.78 ± 0.04</b>
EIG $_{\theta \mathcal{D}_0}$	<b>0.39 ± 0.05</b>	<b>0.45 ± 0.06</b>	0.43 ± 0.04	0.52 ± 0.03
PropScore Error	0.22 ± 0.06	0.2 ± 0.07	0.32 ± 0.06	0.47 ± 0.07
Sample Size	0.18 ± 0.07	0.2 ± 0.06	0.35 ± 0.09	0.41 ± 0.06
CovDist	0.34 ± 0.03	0.3 ± 0.07	0.42 ± 0.08	0.61 ± 0.04